A RIGOROUS ATTEMPT TO VERIFY INTERSTELLAR GLYCINE

L. E. Snyder[1], F. J. Lovas[2], J. M. Hollis[3], D. N. Friedel[1], P. R. Jewell[4], A. Remijan[1,3,5], V. V. Ilyushin[6], E. A. Alekseev[6], and S. F. Dyubko[6]

ABSTRACT

In 2003, Kuan, Charnley, and co-workers reported the detection of interstellar glycine (NH_2CH_2COOH) based on observations of 27 lines in 19 different spectral bands in one or more of the sources Sgr B2(N-LMH), Orion KL, and W51 e1/e2. They supported their detection report with rotational temperature diagrams for all three sources. In this paper, we present essential criteria which can be used in a straightforward analysis technique to confirm the identity of an interstellar asymmetric rotor such as glycine. We use new laboratory measurements of glycine as a basis for applying this analysis technique, both to our previously unpublished 12 m telescope data and to the previously published SEST data of Nummelin and colleagues. We conclude that key lines necessary for an interstellar glycine identification have not yet been found. We identify several common molecular candidates that should be examined further as more likely carriers of the lines reported as glycine. Finally, we illustrate that rotational temperature diagrams used without the support of correct spectroscopic assignments are not a reliable tool for the identification of interstellar molecules.

Subject headings: ISM: abundances - ISM: clouds - ISM: individual (Sagittarius B2[N-LMH], Orion KL, W51 e1/e2) - ISM: molecules - radio lines: ISM

[1]Department of Astronomy, University of Illinois, Urbana, IL 61801
email: snyder@astro.uiuc.edu, friedel@astro.uiuc.edu, aremijan@astro.uiuc.edu

[2]Optical Technology Division, National Institute of Standards and Technology, Gaithersburg, MD 20899-8441
email: lovas@nist.gov

[3]Earth and Space Data Computing Div., Code 930, NASA's Goddard Space Flight Center, Greenbelt, MD 20771
email: Jan.M.Hollis@gsfc.nasa.gov

[4]National Radio Astronomy Observatory, Green Bank, WV 24944-0002
email: pjewell@nrao.edu

[5]National Research Council Resident Research Associate

[6]Institute of Radio Astronomy of NASU, Krasnoznamennaya 4, 61002 Kharkow, Ukraine
email: ilyushin@rian.ira.kharkov.ua; alekseev@rian.ira.kharkov.ua

1. INTRODUCTION

Interstellar glycine (NH_2CH_2COOH) has been unsuccessfully sought using both single-element telescopes (Brown et al. 1979; Hollis et al. 1980; Snyder et al. 1983; Beralis et al. 1985; Guelin & Cernicharo 1989; Combes, Rieu, & Wlodarczak 1996; Ceccarelli et al. 2000) and interferometric arrays (Snyder 1997; Hollis et al. 2003a,b). Recently, Kuan et al. (2003) reported the identification of interstellar glycine (NH_2CH_2COOH) in the direction of the hot molecular cores Sgr B2(N-LMH), Orion KL, and W51 e1/e2.

We note several unusual aspects about the Kuan et al. (2003) reported glycine results. First, their glycine report was based on the detection of 27 spectral line features in the sources Orion KL, W51 e1/e2, and Sgr B2(N-LMH). They used the NRAO[7] 12 m radio telescope operating in the range of 130 to 242 GHz. The sheer number of 27 independent spectral line features detected in 3 different sources appears to suggest overwhelming evidence. Certainly the detection of the same ensemble of spectral lines in multiple sources is a characteristic of interstellar molecules with structural components similar to glycine, such as formic acid (HCOOH) and acetic acid (CH_3COOH)(see, for example, Liu, Mehringer, & Snyder 2001; Remijan et al. 2002). However, each of the three glycine sources was observed to contain no more than 13 to 16 of the 27 independent spectral lines features and only 3 of the 27 spectral line features were found to be common to all 3 sources. Second, 16 of the 27 reported glycine features are not the four-fold degenerate rotational transitions that should be the most likely to be detected for R-branch asymmetric rotor transitions. Third, the glycine rest frequencies used in their observations were based on a Hamiltonian calculation which was extrapolated over 100 GHz. This method can yield potentially large uncertainties in the frequency predictions. Fourth, the glycine column densities derived from rotational temperature diagrams were surprisingly high and of the same order as previously found for structurally similar, but simpler, molecules in these sources (Liu et al. 2001). In fact, Orion KL was reported to have the highest glycine column density, but the interstellar molecule with structure closest to glycine, acetic acid, has never been detected there (Remijan et al. 2003).

In this paper, we investigate the above concerns by starting from new laboratory measurements of glycine that improve the Hamiltonian fit and thereby result in highly reliable interpolated frequency predictions which provide the foundation for our discussion. We list and explain the essential criteria for identifying a new interstellar molecule such as glycine. Then we use these criteria on key glycine spectral lines reported by Kuan et al. (2003) to interpret independent observational data for Orion KL, W51 e1/e2, and Sgr B2(N-LMH), and show that their key lines fail the tests required for a correct glycine identification. In investigating alternative identifications, we find that the carriers of several important spectral lines which have been assigned to glycine are more logically assigned to other, more common species. Finally, we find that random choices of unidentified spectral lines can be used to generate reasonable rotational temperature diagrams

---

[7]The National Radio Astronomy Observatory (NRAO) is a facility of the National Science Foundation operated under cooperative agreement by Associated Universities, Inc.

similar to those published by Kuan et al. (2003).

2. GLYCINE SPECTRAL LINE ANALYSIS AND PREDICTED REST FREQUENCIES

The microwave spectrum of conformer I of glycine was first recorded by Suenram & Lovas (1980) from 82 GHz to 113 GHz in a heated parallel plate Stark cell. This study provided the rotational analysis and rough dipole moment determination. Further measurements of the ^{14}N quadrupole coupling hyperfine structure and Stark effect on low J transitions between 16 GHz and 24.5 GHz were subsequently reported by Lovas et al. (1995). While these literature data provided a firm basis for predicting transitions up to about 150 GHz for guiding past interstellar searches, the 2 σ (standard deviation) uncertainties[8] ranged from 1.5 MHz at 206 GHz to 2.8 MHz at 240 GHz for the main interstellar transitions reported by Kuan et al. (2003). Recently, at Kharkow a heated quartz absorption cell was used to provide new measurements between 75 GHz and 260 GHz utilizing an automated synthesizer-based spectrometer described by Ilyushin et al. (2001). New glycine search frequencies could then be predicted by incorporating both the previously reported transitions and the new measurements into a rotational analysis which employed the Watson A-reduction Hamiltonian with quartic centrifugal distortion terms included (Watson 1977). The details of these laboratory measurements and Hamiltonian calculations will be reported in a future paper. For this paper, it is important to note that for the majority of the calculated transitions the uncertainties have been reduced by a factor of 10 or more from those used by Kuan et al. (2003). Thus, we are starting our analysis with highly accurate glycine rest frequency predictions.

Table 1 summarizes the reported glycine line detections in the direction of the hot molecular cores Sgr B2(N-LMH), Orion KL, and W51 e1/e2. The first column lists a number that Kuan et al. (2003) introduced to represent a particular glycine line. For the convenience of the reader, we adopt this shorthand notation hereafter referred to as the "glycine line number". The second column gives the rotational quantum numbers of the associated transitions, and the third identifies each reported transition as an a-type or a b-type. The fourth column lists our newly calculated glycine rest frequencies, and the fifth and sixth columns give the associated line strengths and upper energy levels. The final six columns in Table 1 list the observed LSR velocity and brightness temperature of each glycine line reported for each source. We have listed in boldface the LSR velocity and brightness temperature values for the lines that were displayed by Kuan et al. (2003).

---

[8]Unless otherwise noted, all uncertainties quoted in this paper are 2 σ or coverage factor k = 2 as described by Taylor & Kuyatt (1994).

3. ESSENTIAL CRITERIA FOR ESTABLISHING THE IDENTIFICATION OF A NEW INTERSTELLAR MOLECULE

The task of establishing the identification of a new interstellar molecule in a dense interstellar clouds is made more complicated by high spectral line densities. For example, at 3 mm wavelength Sgr B2(N-LMH) has a spectral line density of 6.06 lines per 100 MHz, half of which are unidentified (Friedel et al. 2004). This is the highest reported line density in radio astronomy. Hence, the detection of spectral lines with frequencies close to a new species is not in itself sufficient evidence for a correct assignment. Consequently, there are several criteria to consider in securing the correct identification of a new interstellar molecule such as glycine.

Rest Frequencies: The most important criterion for establishing the identification of a new interstellar molecule is that the rest frequencies must be established to a high degree of accuracy. Preferably, the spectral line astronomical rest frequencies to be used in the interstellar search should have been directly measured in the laboratory. If such direct measurements are not available, interpolation fitting of the available laboratory data from other frequencies should allow construction of a high precision Hamiltonian model which can be used to predict search frequencies with uncertainties on the order of 1 part in 10 million.

Frequency Agreement: There must be frequency agreement among all detected transitions. This means that an accurate astronomical rest frequency of the assigned transition must be in reasonable agreement with the frequency corresponding to the LSR velocity of the source. Variations in the LSR velocity of a given molecular species can occur when regions with different kinematics contribute to the emission or absorption spectrum. However, it is evident that emission lines from a given molecular species which emanate from a region with no large kinematic variance will have a well-defined velocity field. Examples are the VLA measurements of the kinematics of methyl formate ($HCOOCH_3$) toward OMC-1 by Hollis et al. (2003a) and ethyl cyanide (CH_3CH_2CN) toward Sgr B2(N-LMH) by Hollis et al. (2003b). If there is a source velocity gradient, as established from observed transitions of known molecules, it cannot be a random function of transition frequency or energy level.

Furthermore, it is not uncommon to have an interstellar spectral line from one species blend with another line of either the same or another species. In order to correctly assign or confirm a line identification, a common standard is that the lines should be at least resolved by the Rayleigh criterion. That is, the minimum distance between two spectral lines in frequency space must be such that the maximum intensity of one line falls on the first null of the other (see, for example, Jenkins & White 1957; Sommerfeld 1964). This is approximately equivalent to requiring that overlapping lines be separated by their full line width at half maximum intensity (assuming identical line profiles). In practice, a more stringent criterion based on the signal-to-noise ratio is often needed whereby two overlapping lines can be considered resolved if they are at least separated at half-maximum intensity of the weakest line.

Beam Dilution: Suppose one uses a single-element radio telescope with circular aperture of

diameter D (such as the NRAO 12 m) to observe separate transitions of some molecule at 50 GHz, 100 GHz, and 150 GHz. The full half-power beam width (HPBW) of the telescope is approximately given by 1.22 λ/D rad (Born & Wolf 1980; see also Rohlfs & Wilson 2000), so in this case the telescope HPBW changes by a factor of 3 over the range of observations. As we will discuss, beam dilution scales with source size squared and beam size squared. To examine the required correction for beam dilution, we can start with $< N_T >$, the beam-averaged molecular column density determined from the integrated intensity of a rotation transition observed by a single-element radio telescope. In autocorrelation mode, with the assumptions of LTE and low optical depth[9] (see, for example, Snyder et al. 2001; Dickens et al. 1997), $< N_T >$ is given by

$$< N_T >= \frac{1.67 \; W_T \; Z \; e^{E_u/T_{rot}}}{S\mu^2\nu} \times 10^{14} \; \text{cm}^{-2}.$$

(1)

In equation (1), $W_T = \int T_R \; dv$ in K km s^{-1}, where T_R is the radiation temperature of the source and dv is the FWHM line width. T_R is related to the measured antenna temperature T_R^* (corrected for atmospheric attenuation, rear spillover, blockage, ohmic losses, and forward spillover) by $T_R = T_R^*/\eta_C$, where η_C is the source-beam coupling efficiency (Kutner & Ulich 1981). Other terms in equation (1) are Z, the rotational partition function, E_u, the upper rotational energy level, T_{rot}, the rotational temperature, S, the line strength, μ^2, the square of the dipole moment in Debye^2, and ν, the frequency in GHz. If the source is comparable to or smaller than the main beam, $\eta_C = \eta_M^* \; B$, where η_M^* is the corrected main beam efficiency and is the fraction of power in the main beam relative to the power in the main beam plus error beam (Jewell 1990). B is the geometric coupling efficiency between the main beam and the source, and is often called the beam filling factor. Note that η_M^* is related to the phase errors of the reflector surface and is thus a function of frequency. For example, for the NRAO 12 m, $\eta_M^* = 0.83$ at 113 GHz and 0.45 at 240 GHz. The above formalism is applicable to sources with angular extent smaller than or on the order of the main beam. Highly extended sources may couple with some or all of the error beam and require a different source-beam convolution.

For a circular Gaussian telescope beam size Θ_b centered on the peak of a circular Gaussian source of size Θ_s, the resulting convolution yields a beam filling factor B given by (e.g., see equation (28) of Ulich & Haas 1976)

$$B = \frac{\Theta_s^2}{\Theta_b^2 + \Theta_s^2}.$$

(2)

---

[9]The corrections to apply when the optical depth is not low and when the excitation is subthermal have been discussed by Goldsmith & Langer (1999), and the aspects of maser excitation have been examined by Reid & Moran (1988). Because we are following the assumptions of Kuan et al. (2003) that their reported glycine lines are optically thin and in LTE, we will confine our discussion to this particular case.

If $\Theta_s \gg \Theta_b$, B $\sim$ 1. When $\Theta_s \sim \Theta_b$, B $\sim$ 0.5, but if $\Theta_s \ll \Theta_b$, B $\sim \frac{\Theta_s^2}{\Theta_b^2}$.

Relative Intensities: Once several molecular transition assignments have been made, their relative intensities must be tested for consistency. For a source comparable to or smaller in angular size than the main beam of the telescope, the relative intensity of two single lines is determined by the corrected beam efficiencies, beam filling factors, dipole moments, line strengths, frequencies, energy levels, and rotational temperature according to equation (1) as

$$\frac{T_R^*(i)}{T_R^*(j)} = \left(\frac{\eta_M^*(i)}{\eta_M^*(j)}\right)\left(\frac{B_i}{B_j}\right)\left(\frac{\nu_i}{\nu_j}\right)\left(\frac{S_i}{S_j}\right)\left(\frac{\mu_i^2}{\mu_j^2}\right) e^{-\frac{E_{ui}-E_{uj}}{T_{rot}}}. \tag{3}$$

Conformer I glycine has an a-type dipole moment, $\mu_a = 0.911(6)$ D ($3.039(20) \times 10^{-30}$ C m), and a b-type, $\mu_b = 0.697(10)$ D ($2.325(34) \times 10^{-30}$ C m) (Lovas et al. 1995). Therefore, for a given frequency, the product $S\mu^2$ dictates that a-type transitions are stronger than b-type when S values are comparable.

A typical property of prolate asymmetric rotors such as glycine is that two low K_{-1} a-type and two b-type transitions become degenerate as the transition frequencies increase. In this four-fold degeneracy, all four transitions have the same rest frequency and energy levels, but different line strengths for the a-type and the b-type. This effect begins at $\sim$ 107 GHz for glycine and it is important because the lines with this degeneracy are the most likely to be detected. The total intensity of a four-fold degenerate line at frequency ν_i is given by the sum of the four individual unresolved components, $\left(\sum_{k=1}^{4} T_R^*(k)\right)_i$, and the ratio of the *ith* degenerate line to the *jth* degenerate line is given by equation (1) as

$$\frac{\left(\sum_{k=1}^{4} T_R^*(k)\right)_i}{\left(\sum_{k=1}^{4} T_R^*(k)\right)_j} = \left(\frac{\eta_M^*(i)}{\eta_M^*(j)}\right)\left(\frac{B_i}{B_j}\right)\left(\frac{\nu_i}{\nu_j}\right)\left(\frac{S_{ai}\mu_a^2 + S_{bi}\mu_b^2}{S_{aj}\mu_a^2 + S_{bj}\mu_b^2}\right) e^{-\frac{E_{ui}-E_{uj}}{T_{rot}}}. \tag{4}$$

Similar expressions can be derived for comparing the intensity of a single glycine line to either a two-fold or a four-fold degenerate glycine line.

Confirming Transitions: Once a candidate line is assigned, the assumption of optical thinness under LTE conditions allows predictions of intensities of additional confirming transitions unless line self-absorption, maser activity, or some other mitigating effect is evident. Hence, a key test of the correctness of the assignment of a transition is that any other transitions connected by favorable transition probabilities must also be present if the relative intensity predictions lead to detectable signal levels.

The maximum line strength for a-type asymmetric rotor R-branch transitions of a molecule like glycine occurs when S approaches J', the upper level value of J. For a-type transitions, this means that the strongest transitions in a series will be those for which $J'_{K'_{-1},K'_1} - J_{K_{-1},K_1} = J'_{0,J'} - J'-1_{0,J'-1}$ or $J'_{1,J'} - J'-1_{1,J'-1}$. The next strongest in this series will be $J'_{1,J'-1} - J'-1_{1,J'-2}$ or $J'_{2,J'-1} - J'-1_{2,J'-2}$. For b-type transitions, the maximum line strength occurs when S approaches $J'-1$. Here the strongest transitions will be those for which $J'_{0,J'} - J'-1_{1,J'-1}$ or $J'_{1,J'} - J'-1_{0,J'-1}$. The next strongest will be $J'_{1,J'-1} - J'-1_{2,J'-2}$ or $J'_{2,J'-1} - J'-1_{1,J'-2}$. Note that a-type transitions follow radiative selection rules where the parity change of the quantum numbers K_{-1},K_1 in a transition is e,e ↔ e,o (even, even ↔ even, odd) or o,o ↔ o,e while the b-type transitions obey e,e ↔ o,o or e,o ↔ o,e (see, for example, Townes & Schawlow 1975).

4. AN EXAMINATION OF THE DATA

Kuan et al. (2003) state that their 27 glycine lines (Table 1) are detected in one or more hot molecular cores (HMCs). We note that HMCs are compact objects where interferometric measurements have shown that structurally similar but simpler large molecules are concentrated with diameters < 10". For example, the HMC of one of their sources, Sgr B2(N-LMH), is ∼ 4" as measured in ethyl cyanide (CH_3CH_2CN) and vinyl cyanide (CH_2CHCN) by Liu & Snyder (1999). On the other hand, Kuan et al. (2003) assume that their HMC glycine lines are optically thin and in LTE and do not correct for beam dilution in their rotational temperature diagrams- a tacit assumption that their glycine sources are extended enough to at least fill their beam. In the case of Orion KL, they speculated that the glycine emission is extended because the rotational temperature diagram has a "tight fit" and, in addition, perhaps the emission is not perfectly centered at the nominal compact ridge position. They used this scenario to reject the Orion glycine negative results found by Combes et al. (1996) with the IRAM 30 m telescope because the narrower 30 m beam might have missed a significant portion of the glycine emission observed by the wider NRAO 12 m beam. The widest 12 m beam used for the Kuan et al. (2003) observations is 45" at the lowest reported frequency in Table 1, 130,346.775 MHz, which corresponds to glycine line 1.

In the following, we will apply the criteria from §3 to examine available observational data for the possibility that the spectral lines assigned to glycine have been misidentified. In order to address the ambiguities introduced by the glycine source sizes, we will assume two cases: (1) the glycine emission sources are HMCs with core diameters typically < 10"; or (2) glycine fills the beam of the 12 m telescope and hence is extended over at least 45" in each source. For our analysis we will use our newly determined astronomical rest frequencies listed in Table 1.

4.1. VLA Searches for Glycine in Compact Sources: Orion and Sgr B2(N-LMH)

In 2001, Hollis et al. (2003b) conducted a deep Q-band ($\lambda \sim 7$ mm) search with the Very Large Array (VLA) toward OMC-1 in four rotational transitions of conformer I glycine. The J2000.0 phase center for their observations was $\alpha = 5^h35^m14^s.25$ and δ = -5°22′35″.5, which is midway between the Orion hot core source and the peak formic acid position of Liu et al. (2002). The Kuan et al. (2003) pointing position precessed from B1950.0 to J2000.0 was $\alpha = 5^h35^m14^s.48$ and δ = -5°22′36″.6 toward Orion KL. The average 12 m telescope half-power beam width (HPBW) for the Orion observations of Kuan et al. (2003) was $\sim$ 41" and the VLA primary beam $\sim$ 45", so the difference in pointing positions is not significant. The best VLA upper limits of Hollis et al. (2003b) were for the $7_{0,7}$ - $6_{0,6}$ transition at 47,753.841(28) MHz with S = 6.851, E_u = 8.657 K, and synthesized telescope beam size $\Theta_b = 6''$: $< N_T > < 8.0 \times 10^{14}$ cm^{-2} for T_{rot} = 43 K; and $< N_T > < 25.2 \times 10^{14}$ cm^{-2} for T_{rot} = 100 K. Kuan et al. (2003) found $< N_T > = 4.37 \times 10^{14}$ cm^{-2} for T_{rot} = 141 K, which is below the upper limits of Hollis et al. (2003b) only if there is no significant beam dilution in the 12 m results for Orion KL. However, if the glycine source size is 6" in diameter (suggested by Hollis et al. 2003b), then the 12 m glycine column density $< N_T >$ becomes 2.08 $\times$ 10^{16} cm^{-2}, which is far above the VLA upper limits.

In 2003, Hollis et al. (2003a) repeated their VLA Q-band glycine search toward Sgr B2(N-LMH). Again the results were negative, and the best upper limits were for the $7_{0,7}$ - $6_{0,6}$ transition observed with synthesized beam 1.″5×1.″4 in the direction of the K2 position. They reached an upper limit of $< N_T > < 1.4 \times 10^{17}$ cm^{-2} for T_{rot} = 170 K. In this same source, Kuan et al. (2003) reported $< N_T > = 4.16 \times 10^{14}$ cm^{-2} for T_{rot} = 76 K, from observations with an average HPBW of 38″. If the glycine source size is comparable to the VLA synthesized beam, then the 12 m glycine column density $< N_T >$ becomes 2.67 $\times$ 10^{17} cm^{-2}, which is again above the VLA upper limits.

In summary, the VLA glycine negative results (Hollis et al. 2003b; 2003a) contradict the glycine detection reports only if the Orion glycine sources in Orion and Sgr B2(N-LMH) are compact. However, as discussed previously, Kuan et al. (2003) assumed that their glycine emission sources are extended and at least 45" in diameter. In the following sections, we will examine this assumption.

4.2. Search for Glycine in Extended Sources: Orion KL

A direct way to examine the assumption of Kuan et al. (2003) that their reported glycine line sources are extended is to use their reported results to generate predicted intensities for other glycine lines that they did not observe. These predictions can be checked against other single-element telescope observations that would be sensitive to glycine emission from extended sources. In particular, we observed interstellar acetone [(CH$_3$)$_2$CO] in 1995 March with the NRAO 12 m radio telescope toward Sgr B2(N) (Snyder et al. 2002). During Orion time, we searched for the nearly four-fold degenerate J = 19-18 glycine transitions around 113,336 MHz. Our Orion KL pointing position was essentially identical to that used by Kuan et al. (2003): exactly the same

right ascension and within 9" in declination. The NRAO 3 mm single-sideband SIS receiver had sideband rejection $\geq$ 25 db and effective system temperature (referenced to above the atmosphere and including rear and forward spillover efficiencies) of $\sim$ 300 K. Chopper calibration corrected for atmospheric extinction and telescope losses and the resultant data are on the T_R^* temperature scale (Kutner and Ulich 1981). Data were taken while position switching 30' in azimuth, while Kuan et al. (2003) switched by 20'. The half power beam width (FWHM) was $\sim$56" at 113.3 GHz. The spectrometer consisted of the NRAO Hybrid Spectrometer with two 256 channel filter banks used as a backup. The Hybrid Spectrometer was operated with two polarization IFs in parallel, with 300 MHz bandwidth and 768 Hanning-smoothed channels per IF, giving an effective spectral resolution of 0.781 MHz. The filter banks were operated with two IFs in parallel, with 250 kHz resolution in one bank and 500 kHz in the other. Therefore, this system was exactly the same as that used by Kuan et al. (2003) except that they chose to use wider filters for their observations. The NRAO 12 m data were reduced using the NRAO data reduction package UniPOPS (Salter, Maddalena, & Garwood 1995) [10].

The Kuan et al. (2003) pointing position toward Orion KL was α(B1950.0) = $5^h32^m47^s.0$ and δ(B1950.0) = -5°24'30".0. Our pointing position was α(B1950.0) = $5^h32^m47^s.0$ and δ(B1950.0) = -5°24'21".0, which in our $\sim$ 56" beam was only a negligible 9" difference. Table 2 summarizes our Orion KL search frequencies for the J = 19-18 glycine transitions and for the test lines used to check the operation of the system. The first column lists rest frequencies; the second and third list molecular identifications (when known) and rotational quantum numbers; the fourth, fifth, and sixth columns give the transition types, line strengths, and upper energy levels; and the next two columns give intensities and line widths for Orion KL. Figure 1 shows the Orion KL spectra from 113,323 to 113,354 MHz (centered at 113,339 MHz) observed with the Hybrid Spectrometer on the NRAO 12 m. The spectral positions of the negative results for the nearly four-fold degenerate J = 19-18 glycine lines (listed in Table 2) are marked by the four vertical lines. The unidentified line U113.226 is on the left, and the 6_1-6_0 E_1 transition of CH_3OD is on the right; these two lines served as system checks.

Kuan et al.(2003) reported the detection of 15 optically thin glycine lines in the direction of Orion KL. If they were glycine, lines 1, 5, 6, 8, 9, 14, 15, 16, 17, 18, and 25 in Table 1 would be single transitions. Lines 11, 21, 24, and 26 would be four-fold degenerate. Of these 15 lines, none contained connecting confirming transitions, which would be a key test of the correctness of the glycine assignment as discussed in §3. Among these, we note that lines 5, 14, 15, 16, and 26 marginally meet the Rayleigh criterion for spectral resolution. By applying the discussion in §3 and adapting equation 4 to *each* of the reported Orion glycine lines, we can use each reported line to make an independent prediction of the intensity of the nearly four-fold degenerate J = 19-18 glycine lines that we did not detect, as shown in Figure 1. Figure 2 shows the range of predicted intensities that we should have observed with the NRAO 12 m telescope for each of the 15 of the

---

[10]UniPOPS information is available at http://www.gb.nrao.edu/~rmaddale/140ft/unipops/unipops_toc.html.

reported Orion glycine transitions emanating from a 45" extended source. For each prediction, three different points are labeled to denote the Kuan et al. (2003) rotational temperature and its uncertainties, $T_{rot} = 141^{+76}_{-37}$ K. The uncertainties for each rotational temperature point are based on the rms noise level given for each reported glycine line by Kuan et al. (2003) (see Table 1). The dotted line in Figure 2 shows the 3.7 mK noise level from Figure 1. For example, Orion line 21 has a peak intensity $T_R^* = 230\pm 10.0$ mK as observed with a 30" beam. In Table 1, it is assigned as a degenerate quartet of two a-type and two b-type glycine lines at 206,468 MHz: $35_{0,35}$-$34_{0,34}$; $35_{1,35}$-$34_{1,34}$; $35_{0,35}$-$34_{1,34}$; and $35_{1,35}$-$34_{0,34}$. If line 21 is an optically thin glycine line in LTE with a rotational temperature of 141 K, then the nearly blended J = 19 - 18 quartet would appear in Figure 1 with peak intensity $T_R^* \sim 143$ mK $\pm$ 7 mK for an extended source size of $\Theta_s = 45$". All of the predictions plotted in Figure 2 are above the 3.7 mK noise level from Figure 1. Hence, if the Orion reported glycine detection were correct, we should have detected a blended line with intensity 5 mK $\leq T_R^* \leq 205$ mK for the J = 19 - 18 glycine quartet. Since we did not, we conclude that glycine has not been detected in an extended source in Orion KL. In §4.1, we ruled out the detection of glycine in a compact source in Orion. Consequently, we conclude that the presence of interstellar glycine has not been verified in Orion KL.

4.3. Search for Glycine in Extended Sources: W51

During the 1995 March observations with the NRAO 12 m, we also searched for the four-fold nearly degenerate J = 19 - 18 glycine transitions in the direction of W51. The Kuan et al. (2003) pointing position toward W51 e1/e2 was α(B1950.0) = $19^h21^m26^s.3$ and δ(B1950.0) = $+14°24'39".0$. Our W51 pointing position was α(B1950.0) = $19^h21^m26^s.3$ and δ(B1950.0) = $+14°24'43".0$, which in our $\sim$ 56" beam was only a negligible 4" difference. As with the Orion KL observations, our W51 data were taken while position switching 30' in azimuth, while Kuan et al. (2003) switched 20'. Again, the system was exactly the same as that used by Kuan et al. (2003) except that they used wider filters. In Table 2, the last two columns give intensities and line widths for the W51 search frequencies for the J = 19-18 glycine transitions and for the test lines used to check the operation of the system; they are the same transitions used for the Orion KL search. Figure 3 shows the W51 spectra from 113,323 to 113,354 MHz (centered at 113,339 MHz) observed with the Hybrid Spectrometer on the NRAO 12 m. As in the case of Orion KL, the spectral positions of the negative results for the nearly four-fold degenerate J = 19-18 glycine lines (listed in Table 2) are marked by the four vertical lines centered at 113,336 MHz. As in Figure 1, the system checks are the unidentified line U113.226 on the left, and the weak 6_1-6_0 E_1 transition of CH_3OD on the right.

Kuan et al.(2003) reported the detection of 16 optically thin glycine lines in the direction of W51. If these lines were glycine, lines 3, 4, 5, 7, 8, 9, 13, 15, and 25 in Table 1 would be single transitions. Line 12 would be two-fold degenerate and lines 19, 20, 21, 24, 26, and 27 would be four-fold degenerate. Of these 16 lines, none contained connecting confirming transitions, which

would be a key test of the correctness of the glycine assignment as discussed in §3. Among the displayed spectra, line 27 does not meet the Rayleigh criterion for spectral resolution. As with the Orion KL data, we can use the intensity of each of the reported glycine lines to independently predict the intensity of the nearly four-fold degenerate J = 19-18 glycine lines at 113,366 MHz that we did not detect, as shown in Figure 3. Figure 4 shows the range of predicted intensities that we should have observed with the NRAO 12 m telescope for each of the 16 reported W51 glycine transitions emanating from a 45" extended source. As in Figure 2, three different points are labeled for each prediction to denote the Kuan et al. (2003) rotational temperature and its uncertainties, $T_{rot} = 121^{+71}_{-32}$ K. The uncertainties for each rotational temperature point are based on the rms noise level given for each reported glycine line by Kuan et al. (2003) (see Table 1). The dotted line in Figure 4 shows the 6.4 mK noise level from Figure 3. All of the predictions plotted in Figure 4, except those from line 19, are above the this noise level. Hence, the intensities of 15 out of 16 glycine lines predict that we should have detected a blended J = 19 - 18 glycine line quartet with intensity 10 mK $\leq T^*_R \leq$ 105 mK if the reported W51 glycine detection is correct. Since we did not, we conclude that the presence of interstellar glycine has not been verified in W51.

4.4. Search for Glycine in Extended Sources: Sgr B2(N-LMH)

Kuan et al.(2003) assigned glycine transitions to 13 emission lines in the direction of Sgr B2(N-LMH) at α(B1950.0) = $17^h44^m10^s.20$ and δ(B1950.0) = -28°21'15".0. Their rest frequencies were calculated with respect to V_{LSR} = 64 km s^{-1}. Their emission lines 1, 2, 6, and 7 in Table 1 were assigned to single glycine transitions. Line 10 would have a five-fold degeneracy and line 12 a two-fold if they were glycine. Lines 19, 20, 21, 22, 23, 24, and 26 would be four-fold degenerate. Of these 13 lines, only lines 21 and 22 would contain connecting confirming transitions, a key test of the correctness of the assignment as discussed in §3. Only lines 19, 20, 21, 23, and 26 were displayed by Kuan et al. (2003); of these, lines 19, 21, and 23 marginally meet the Rayleigh criterion for spectral resolution. Fortunately, Nummelin et al. (1998) surveyed Sgr B2(N) in the direction α(B1950.0) = $17^h44^m10^s.10$ and δ(B1950.0) = -28°21'17".0 between 218.3 and 263.55 GHz with the 15 m Swedish ESO-Submillimetre Telescope (SEST). Their position coincided with the Sgr B2(N-LMH) position used by Kuan et al. (2003). Their beam width was ~ 20" (adequate for extended sources), and their frequency range covered several important glycine transitions, which we will discuss. Their rest frequencies were calculated with respect to V_{LSR} = 62 km s^{-1}.

By applying the discussion in §3 to predict the expected glycine intensities, it is straightforward to use the Nummelin et al. (1998) data to examine the Sgr B2(N-LMH) glycine assignments of Kuan et al. (2003). If lines 26 and 27 were glycine, for any reasonable temperature their line strengths would make them the the two strongest glycine lines in Table 1. Line 26 was observed by Kuan et al. (2003) with the NRAO 12m telescope to have T^*_R = 94 mK. It was assigned to a degenerate glycine quartet consisting of two a-type and two b-type transitions with J = 40 - 39, K_{-1} = 1 or 2 at 240,899.5 MHz. Nummelin et al. (1998) detected this line with SEST; it

has a main beam brightness temperature $T_{mb} = 300$ mK. Kuan et al. (2003) assigned line 27 to a degenerate glycine quartet with J = 41 - 40, $K_{-1} = 0$ or 1 at 241,373.3 MHz. While line 27 would be expected to be slightly stronger than line 26, it was reported by Kuan et al. (2003) to be masked by unidentified interlopers in their Sgr B2(N-LMH) 12m data and the spectrum was not displayed. However, this interloper masking argument is not supported by the data of Nummelin et al. (1998), which show not only that the line 27 frequency falls in a relatively clear spectral region in Sgr B2(N-LMH), but also that line 27 was not detected (as we will discuss).

Nummelin et al. (1998) reported all of their data in units of K on the main beam brightness temperature (T_{mb}) scale. Hence, η_M^*, the main beam efficiency has already been taken into account, and equation 4 may be used for intensity predictions with T_{mb} substituted for T_R^*/η_M^*. To conduct our analysis, we used the $T_{mb} = 300$ mK intensity (with an estimated 50 mK rms noise level uncertainty) of line 26 from Nummelin et al. (2003) as a basis for predicting the intensities of those $K_{-1} = 1$ or 2 degenerate glycine quartet lines connected to line 26 via two a-type and two b-type transitions. By confining our predictions to the Nummelin et al. (1998) data set, we eliminated any problems caused by calibration differences between the NRAO 12 m and SEST telescopes. Table 3 lists all of the $K_{-1} = 1$ or 2 degenerate glycine lines that fall in the 218.3 - 263.55 GHz range of the Nummelin et al. (1998) survey that would be radiatively connected to line 26 if its assignment to the degenerate glycine quartet of two a-type and two b-type transitions with J = 40 - 39, $K_{-1} = 1$ or 2, were correct. The first column lists the individual quantum numbers of each degenerate frequency group, the second lists the transition type, and the third lists the rest frequency of each degenerate glycine line. Note that the line quartets are arranged in descending order of frequency. The top transition in each degenerate quartet feeds directly into the top transition in the next lower frequency degenerate quartet, the second transition in each degenerate quartet feeds directly into the second transition in the next lower degenerate quartet, etc. The fourth column in Table 3 gives the line strengths and the fifth the upper state energy levels. The next column gives the predicted values of T_{mb} for each line if the assignment of line 26 to the J = 40 - 39, $K_{-1} = 1$ or 2, degenerate glycine transition at 240,899.5 MHz were correct. These predicted T_{mb} values (as well as the values for the upper and lower error bars) were calculated for a gas rotational temperature of 75 K with an uncertainty ranging from 59 K to 104 K (Kuan et al. 2003) in addition to the 50 mK rms noise level uncertainty for line 26. The next column lists what was observed by Nummelin et al. (1998) at each frequency: the peak T_{mb} value for any clearly resolved line; the upper limit to the noise level if no line is present; or the notation ... indicating that the line is masked by the wings of an interloper line. The final column in Table 3 lists relevant comments, if any, for each observed frequency. Table 4 follows the format of Table 3 for the stronger $K_{-1} = 0$ or 1 degenerate glycine lines that fall in the same range of the Nummelin et al. (1998) survey. Again, the predicted intensities in Table 4 are based on the observed intensity of $T_{mb} = 300$ mK for line 26 (with an estimated 50 mK rms noise level uncertainty) and the assumption that it can be assigned to glycine.

Examination of Table 3 shows that the $K_{-1} = 1$ or 2 frequencies of the degenerate glycine quartets J = 43 - 42, 38 - 37, and 37 - 36 are obscured by the wings of lines previously identified by

Nummelin et al. (1998). U235.085 at 235,085 MHz would be a possible candidate for the $J = 39$ - 38, $K_{-1} = 1$ or 2, degenerate glycine transition at 235,084.8 MHz, but the peak intensity is low. Finally, the glycine lines missing from the Nummelin et al. (1998) data at the ~ 100 mK level are the $K_{-1} = 1$ or 2 frequencies of the degenerate glycine quartets $J = 42$ - 41 at 252,531.295 MHz and 41 - 40 at 246,716.164 MHz. The data for these missing lines and for line 26 at 240,900.647 MHz are shown in Figures 5(a), 5(b), and 5(c), adapted from the Sgr B2(N) data and molecular assignments of Nummelin et al. (1998).

Table 4 shows that the $K_{-1} = 0$ or 1 frequencies of the degenerate glycine quartets $J = 40$ - 39, 39 - 38, and 38 - 37 are obscured by the wings of lines previously identified by Nummelin et al. (1998). In addition, the spectral region around the degenerate glycine transition $J = 44$ - 43 at 258,820.597 MHz is dominated by what appears to be narrow, weak interference spikes in the Nummelin et al. (1998) data for Sgr B2(N), Sgr B2(M), and Sgr B2(NW). The $K_{-1} = 0$ or 1 glycine lines missing from the Nummelin et al. (1998) data at the ~ 50 mK level are the $J = 43$ - 42 degenerate quartet at 253,005.255 MHz. Furthermore, the $J = 42$ - 41 degenerate quartet at 247,189.500 MHz and the $J = 41$ - 40 degenerate quartet at 241,373.340 MHz (line 27 of Kuan et al. 2003) are missing at the ~ 100 mK level. The data for these missing lines are shown in Figures 5(d), 5(e), and 5(f).

Because of the five missing key quartets summarized in Tables 3 and 4 and shown in Figure 5, we conclude that glycine has not been detected in an extended source in Sgr B2(N). In §4.1, we ruled out the detection of glycine in a compact source in Sgr B2(N-LMH). Thus, we conclude that the presence of interstellar glycine has not been verified in Sgr B2(N).

4.5. Alternative Identifications

Now that we have shown that the carriers of key spectral lines assigned to glycine by Kuan et al. (2003) can not be verified as interstellar glycine, in this section, we suggest some logical assignments to other, more common species. Our proposed carriers are listed in Table 5. The first and second columns list the line number and rest frequency reported by Kuan et al. (2003). The third, fourth, and fifth columns list the possible molecular candidates, the quantum numbers, and rest frequencies of their transitions. The last column gives the sources where the lines were reported. Our proposed carriers are presented to underline the growing impact of line confusion on the difficult problem of identifying new interstellar species. In the following, we discuss the suggested identifications in Table 5 with the caveat that they will have to be substantiated by further observational work.

In §1, we pointed out that one of the peculiarities in the glycine detection report of Kuan et al. (2003) was that each of their three glycine sources (Orion, W51 e1/e2, and Sgr B2(N-LMH)) was observed to contain no more than 13 to 16 of the 27 independent spectral lines features and only 3 of the 27 spectral line features were found to be common to all three sources: lines 21,

24, and 26 in Table 1. Consequently, we will begin with a discussion of lines 21 and 24. Line 21 was observed with the NRAO 12 m telescope with a 30" beam, and was misassigned to the four-fold degenerate glycine quartet $35_{0,35}$-$34_{1,34}$, $35_{1,35}$-$34_{1,34}$, $35_{0,35}$-$34_{0,34}$, and $35_{1,35}$-$34_{0,34}$ at 206,468 MHz. In all 3 sources, line 21 is anomalously strong relative to all other purported glycine transitions that were observed. This suggests that even in the unlikely event that all the other lines reported by Kuan et al. (2003) belong to the same species, then line 21 most likely belongs to another molecular species altogether. We propose that a likely carrier of line 21 is vibrationally excited ethyl cyanide (CH_3CH_2CN) which has recently been shown to be a common constituent of Sgr B2(N-LMH) (Mehringer et al. 2004). The $23_{6,18}$ - $22_{6,17}$ A and E and $23_{6,17}$ - $22_{6,16}$ A and E transitions of vibrationally excited ethyl cyanide (ν_b=1) span the range of 206,466.6 to 206,467.3 MHz (J. C. Pearson, private communication) and would be a logical assignment for line 21. Line 24 was misassigned to the nearly four-fold degenerate glycine quartet $36_{3,33}$-$35_{4,32}$, $36_{4,33}$-$35_{4,32}$, $36_{3,33}$-$35_{3,32}$, and $36_{4,33}$-$35_{3,32}$ at an average observed frequency of 228,418.8 MHz. Kuan et al. (2003) dismissed the frequency coincidence of the J = 24 - 23, K=11 transition doublet of vinyl cyanide (CH_2CHCN) at 228,418.1 MHz as an "unlikely" ν=2 state of the molecule. However, these transitions are actually in the ν_{15}=1 state, which Nummelin & Bergman (1999) have shown to be common for vinyl cyanide emission as observed with the SEST 15m telescope in SgrB2(N). Thus, line 24 is most likely ν_{15}=1 vinyl cyanide, a common constituent of interstellar clouds. Finally, we note that the third key line, line 26, has the same flux ($\sim$ 6 Jy) in the $\sim$ 20" beam of Nummelin et al. (1998) as it has in the $\sim$ 26" beam of Kuan et al. (2003). This suggests that the carrier of line 26 will also be a constituent of a somewhat compact source, such as a hot molecular core.

In addition to lines 21 and 24, we have examined potential carriers for 7 other reported glycine lines that were detected in only one or two of the three glycine sources. These will be discussed in order of frequency as they are listed in Table 5. Line 6 is very close to a favorable transition of $HCOOCH_3$ (methyl formate[11]), a molecule found in abundance in both Sgr B2(N) and Orion. Line 7 is near favorable transitions of CH_2CDCN (deuterated vinyl cyanide[11]) and H_2CCCC (butadiynyl radical). Line 8 is near c-$C^{13}CCH_2$ (cyclopropenylidene[11]). Line 10 is almost coincident with g-CH_3CH_2OH (gauche ethanol) in the ground state. Kuan et al. (2003) misidentified this as a ν = 1 vibrationally excited state of ethanol. The frequency of line 12 agrees almost exactly with a likely transition of $CH_2DCH_2CN^{[11]}$. Line 13 is almost coincident with transitions of both ethyl cyanide[12] and acetone (($CH_3)_2CO$). The ethyl cyanide line is actually in the ν_{15}=1 state, not ν=2 as noted by Kuan et al. (2003). Finally, the frequency of line 16 agrees almost perfectly with the 2 listed transitions of acetone[12]. In summary, there are good alternative candidates for 9 of the lines reported as glycine that are more likely to be detectable than glycine. These alternatives can easily be checked by further observational work.

---

[11]Also noted by Kuan et al. (2003) as a possible line carrier candidate, but dismissed without further consideration.

[12]Listed as "unlikely" by Kuan et al. (2003), but should still be considered as a line carrier candidate unless ruled out by further observations.

5. GLYCINE ROTATIONAL TEMPERATURE DIAGRAMS

Kuan et al. (2003) used rotation temperature diagrams constructed from Sgr B2(N-LMH), Orion KL, and W51 e1/e2 data to bolster their arguments for the identification of glycine. In Appendix A, we have noted that rotational temperature diagrams can not be used as independent tools to verify interstellar spectral line identifications because the frequency parameter in equation A4 or A5 will dominate the integrated intensity, line strength, and dipole moment terms for typical spectral line data in the millimeter or submillimeter range. In the following discussion, we illustrate this important point with two molecular examples: chlorine nitrate (^{35}ClONO$_2$), a molecule which is unlikely to be detected in the interstellar medium with current telescopes, and glycine. The chlorine nitrate rest frequencies were calculated from the data of Suenram & Lovas (1984). As a data base, we used the 123 unidentified (U) lines detected with the BIMA Array by Friedel et al. (2004) toward Sgr B2(N-LMH) at 3 mm wavelength. We searched this U line data base for apparent transitions of chlorine nitrate and glycine with the following criteria for matching lines:

1. The 2σ frequency uncertainty of each calculated chlorine nitrate and glycine transition had to be less than 2.82 MHz (equivalent to twice the largest 1σ uncertainty from Kuan et al. 2003). This uncertainty turned out to be less than 1.04 MHz for chlorine nitrate and less than 1.84 MHz for glycine.

2. Friedel et al. (2004) established the rest frequency of each U line by assuming a v_{LSR} of 64 km s^{-1}. Kuan et al. (2003) allowed the velocity range of their reported glycine lines to range between 58 and 75 km s^{-1}. Therefore, we allowed a tolerance in our U line frequencies which corresponded to a v_{LSR} of 64^{+11}_{-6} km s^{-1} with an additional uncertainty of $\pm$ 390 kHz due to the spectral resolution used by Friedel et al. (2004) for the U line observations.

3. The width of each matched U line had to be between 2.8 and 12.7 km s^{-1}, which is the spread in line widths from the data in Kuan et al. (2003) toward Sgr B2(N). There were 2 exceptions to this with ^{35}ClONO$_2$ and 2 with glycine, but the uncertainties easily reached into this range.

4. We selected only U lines whose intensity was not too great for the associated transition. If the U line appeared to be a blend of transitions from several species, it was not used.

Table 6 lists the chlorine nitrate, glycine, and U line frequencies that will be used in our discussion of rotational temperature diagrams. The first two columns list calculated rest frequencies and the corresponding transitions. The third column lists U lines which were selected using the four criteria listed above. The last column contains relevant comments. From our search, 8 U lines matched 15 degenerate and nondegenerate chlorine nitrate transitions and 11 U lines matched 13 degenerate and nondegenerate glycine transitions. These are the lines listed in Table 6 where calculated frequencies of chlorine nitrate and glycine (first column) are paired with specific U lines (third column). Using these calculated frequencies in equation A4 and assuming no beam dilution, a

rotational temperature diagram was constructed for each species which gave rotational temperatures and total column densities. Figure 6 shows the rotational temperature diagram for chlorine nitrate which gives a total column density[13], $< N_T >$, of 2.5(6)x10^{17} cm^{-2} and a rotational temperature of 54(8) K. Figure 7 shows the rotational temperature diagram for glycine, which gives a total column density, $< N_T >$, of 8.5(9)x10^{16} cm^{-2} and a rotation temperature of 79(9) K. While these diagrams and rotation temperatures look reasonable, they do not signify detections, nor are they supporting evidence of detections. We can see how improbable the results are by examining the total column densities. For chlorine nitrate, the total column density is far too large and nearly equivalent to that of methanol (CH_3OH) in Sgr B2(N-LMH) found by Pei et al. (2000). For example, if we assume that the H_2 column density is 1-8x10^{25} toward Sagittarius B2(N) (Kuan, Mehringer, & Snyder 1996; Lis et al. 1993), the chlorine nitrate column density gives a relative abundance of 0.3-2.5x10^{-8}. Schilke, Phillips, & Wang (1995) state that HCl should contain 1/3 of the gas phase Cl and Zmuidzinas et al. (1995) give the relative abundance of HCl toward Sagittarius B2(N) as $\sim$10^{-9}. This would mean that if we believed our rotational temperature diagram results, chlorine nitrate would be 3-25 times more abundant than HCl, an obviously ludicrous conclusion. While the rotational temperature for glycine derived from randomly coincident U lines may seem to agree with Kuan et al. (2003), the total column density is more than two orders of magnitude greater.

Finally, we note that in the frequency range that we searched, the rotational temperature diagram results predicted several strong transitions of both chlorine nitrate and glycine that should have been detected by Friedel et al.(2004), but were not. These lines are noted in Table 6 where the third column lists "None" to signify that no U line (which corresponded to either a chlorine nitrate or a glycine calculated frequency) was detected. For each of these lines, the notes give the minimum expected intensity (in σ) relative to the rms noise level of the spectral window in which each should appear. Each minimum expected intensity was calculated by taking the predicted total column density and rotation temperature for the appropriate species and calculating the column density of the upper state of the transition. From this the integrated line intensity (W_I from equation A4) was found. This was then divided by 12.7 km s^{-1} (the largest line width allowed) giving the minimum expected peak intensity in Jy beam^{-1}. This peak intensity was then divided by the rms noise level (assumed to be 1 σ) in the appropriate spectral window to give the minimum expected intensity in units of σ. These missing strong lines of chlorine nitrate and glycine reinforce the fact that rotational temperature diagrams used without adequate spectroscopic evidence supporting the molecular identification can lead to incorrect results.

We conclude that these rotational temperature diagrams can not provide reliable independent supporting evidence for interstellar molecular identifications because, particularly for weak lines, equation A4 will be dominated by $1/\nu^3$. Conversely, for any "forest" of weak lines spread across a large enough frequency band, one can construct a reasonable looking rotation diagram for any species, even one as unlikely as interstellar chlorine nitrate.

---

[13]The column density and temperature uncertainties are 1σ from the weighted least squares fit.

6. CONCLUSIONS

As we discussed in §1, there are several pecularities if the lines reported by Kuan et al. (2003) in Sgr B2 (N-LMH), Orion KL, and W51el/e2 belong to interstellar glycine. Therefore, we examined their assignments of key glycine transitions to the spectral lines listed in Table 1. We noted that their lack of correction for beam dilution amounted to the tacit assumption that their glycine sources have an extended source size with $\Theta_s \geq 45$". In Orion KL, we found that none of the 15 glycine line assignments could be verified because the reported intensities of all 15 lines predict that a major glycine quartet (J=19-18, $K_{-1} = 0$ or 1) should have been detected in our Orion data from the NRAO 12 m telescope (Figures 1 and 2). So we can conclude that the Orion spectral lines reported by Kuan et al. (2003) (column 8, Table 1) are not glycine. Previously, the VLA data of Hollis et al. (2003a) established upper limits in Orion for compact glycine sources. Therefore, glycine has not been verified in either extended or in compact sources in Orion. In W51el/e2, 16 lines were assigned to glycine. Fifteen of the 16 line intensities lend to the predictions that the J=19-18, $K_{-1} = 0$ or 1 glycine quartets should have been detected in our W51 data from the NRAO 12 m telescope (Figures 3 and 4). Since our spectra show a negative result, we can conclude that the reported W51 spectral lines are also not glycine (column 9, Table 1). In the direction of Sgr B2 (N-LMH), only 13 lines were assigned to glycine but the situation is slightly more complicated by the high spectral line density. However, it can be simplified by recognizing that, based on both line strength values and intensity calculations, the two strongest glycine lines should be those assigned to lines 26 and 27 in column 7 of Table 1. Line 26 appears with a peak intensity of 300 mK in the Sgr B2(N) band scan data of Nummelin et al. (1998), but the important connected lines, J=42-41 and 41-40 in the $K_{-1} = 1$ or 2 series, are missing altogether (Table 3). Furthermore, line 27 should be stronger than line 26, but it too is missing, along with the connected J=43-42 and 42-41 lines in the $K_{-1} = 0$ or 1 series (Table 4). All of these key glycine lines strongly connect major $K_{-1} = 0$, 1, or 2 rotational levels, so their absence is not possible if the other Sgr B2(N-LMH) glycine lines are assigned correctly. Therefore, we conclude that the Sgr B2(N-LMH) spectral lines reported by Kuan et al. (2003) (column 7, Table 1) are not glycine. Furthermore, the VLA data of Hollis et al. (2003) established upper limits for compact glycine sources in Sgr B2(N-LM). Consequently, glycine has not been verified in Sgr B2(N-LMH) either in extended or in compact sources.

If the 27 lines reported by Kuan et al. (2003) in Orion KL, W51el/e2, and Sgr B2(N-LMH) are not glycine, what are they? Lines 21, 24, and 26 in Table 1 are the 3 lines reported to be common to all 3 sources. We have argued that vibrationally excited ethyl cyanide (CH_3CH_2CN) is a logical assignment for line 21, and vibrationally excited vinyl cyanide (CH_2CHCN) for line 24. The intensity of line 26 increases as the observational beam width narrows, so it could also be a vibrationally excited transition of a common interstellar species. Seven other lines could be partially or completely assigned to be common species listed in Table 5. Beyond this, it is difficult to comment on other possible line carrier candidates because Kuan et al. (2003) only published sample spectra for 11 of their 27 lines. Finally, we have demonstrated that rotational temperature diagrams can not by themselves be used to identify interstellar molecules.

APPENDIX A

SOME COMMENTS ABOUT ROTATIONAL TEMPERATURE DIAGRAMS

The conventional method for forming a rotational temperature diagram is to plot the logarithm of normalized column density vs. upper state rotational energy level. However, this approach incorporates several assumptions. First, it is assumed that each region in the interstellar cloud has uniform physical conditions and that the populations of the energy levels can be characterized by a Boltzmann distribution. Second, optically thin conditions are assumed but it may be possible to correct for this assumption later in the analysis. Third, if it is not possible to measure the source size, it must be assumed the source fills the observational beam. So, if the population distribution can be adaquately described by a single rotational temperature and if all the lines are optically thin, the measured fluxes are proportional to the column densities in the upper levels of the transitions being observed.

For autocorrelation (single-element telescope) observations, we can start with equation (1) in §3. For cross-correlation (interferometric array) observations, we can use (see, for example, Snyder et al. 2001)

$$< N_T >= \frac{2.04 \; W_I \; Z \; e^{E_u/T_{rot}}}{B\theta_a\theta_b S\mu^2\nu^3} \times \; 10^{20} \; cm^{-2}. \tag{A1}$$

In equation (A1), $W_I = \int I_\nu dv$ in Jy beam^{-1} km s^{-1}, and I_ν is the flux density per beam. Z is the rotational partition function, B is the beam filling factor, θ_a and θ_b are the FWHM synthesized beam dimensions in arcsec, S is the linestrength, μ^2 the square of the dipole moment in Debye^2, and ν is the frequency in GHz. The beam-averaged upper level column density, $< N_u >$, is defined by

$$\frac{< N_u >}{g_u} = \frac{< N_T >}{Z}e^{-\frac{E_u}{T_{rot}}}, \tag{A2}$$

where g_u is the statistical weight of the upper level (2J+1). A standard approach is to take the Naperian (base e) logarithm of equation (A2),

$$\ln\left(\frac{< N_u >}{g_u}\right) = -\frac{E_u}{T_{rot}} + ln\left(\frac{< N_T >}{Z}\right). \tag{A3}$$

Then for cross-correlation data, equations (A1) and (A3) give

$$\ln\left(\frac{<N_u>}{g_u}\right) = \ln\left(\frac{2.04\ W_1 10^{20}}{B\theta_a\theta_b S\mu^2\nu^3}\right) = -\frac{E_u}{T_{rot}} + \ln\left(\frac{<N_T>}{Z}\right). \qquad (A4)$$

A linear least-squares fit to equation (A4) can be used to construct a rotational temperature diagram where the slope gives the negative reciprocal of the rotational temperature. This temperature can be used to estimate the total molecular column density $< N_T >$. The rotational temperature will be equal to the kinetic temperature only at sufficiently high densities. If the emission is not optically thin, the finite opacity produces an underestimate in the upper level column density of the observed transition and it can also produce an error in the rotational temperature (Goldsmith & Langer 1999). If the opacity can be calculated, corrections can be made to the rotational temperature and total column density. A similar approach can be followed with equations (1) and (A2) to construct a rotational temperature diagram from autocorrelation (single-element telescope) data:

$$\ln\left(\frac{<N_u>}{g_u}\right) = \ln\left(\frac{1.67\ W_T 10^{14}}{BS\mu^2\nu}\right) = -\frac{E_u}{T_{rot}} + \ln\left(\frac{<N_T>}{Z}\right). \qquad (A5)$$

There are two more important caveats about rotational temperature diagrams that must be noted. First, if common (Briggsian) base 10 logarithms are used, the result is

$$\log_{10}\left(\frac{<N_u>}{g_u}\right) = -\frac{E_u\ log_{10}e}{T_{rot}} + \log_{10}\left(\frac{<N_T>}{Z}\right). \qquad (A6)$$

This approach slightly complicates the rotational temperature term. However, it makes the data scatter appear to be smaller since $log_{10}\frac{<N_u>}{g_u} = 0.434\ ln_e\frac{<N_u>}{g_u}$. The second important caveat is in either equations (A4) or equation (A5), the frequency parameter will dominate the integrated intensity, line strength, and dipole moment terms for typical spectral line data in the millimeter or submillimeter range. Hence, rotational temperature diagrams can not be used as independent tools to verify interstellar spectral line identifications. This point is illustrated in §5.

REFERENCES

Berulis, I. I., Winnewisser, G., Krasnov, V. V., & Sorochenko, R. L. 1985, Sov. Astron. Lett. 11, 251

Born, M., & Wolf, E. 1980, Electromagnetic Theory of Propagation Interference and Diffraction of Light (6th ed.; New York: Pergamon Press), 397

Brown, R. D., Godfrey, P. D., Storey, J. V. W., Bassez, M.-P., Robinson, B. J., Batchelor, R. A., McColloch, M. G., Rydbeck, O. E. H., & Hjalmarson, Å. G., 1979, MNRAS, 186, 5P

Ceccarelli, C., Loinard, L., Castets, A., Faure, A., & Lefloch, B. 2000, A&A, 362, 1122

Combes, F., Nguyen-Q-Rieu, & Wlodarczak, G. 1996, A&A, 308, 618

Dickens, J. E., Irvine, W. M., Ohishi, M., Ikeda, M., Ishikawa, S., Nummelin, A., & Hjalmarson, Å. 1997, ApJ, 489, 753

Friedel, D. N., Snyder, L. E., Turner, B. E., & Remijan, A. 2004, ApJ, 600, 234

Goldsmith, P. F., & Langer, W. D. 1999, ApJ, 517, 209

Guelin, M., & Chernicharo, J. 1989, in The Physics and Chemistry of Interstellar Molecules, ed. G. Winnewisser & T. Armstrong, (Berlin: Springer-Verlag), 337

Hollis, J. M., Pedelty, J. A., Snyder, L. E., Jewell, P. R., Lovas, F. J., Palmer, P., & Liu, S.-Y. 2003a, ApJ, 588, 353

Hollis, J. M., Pedelty, J. A., Boboltz, D. A., Liu, S.-Y., Snyder, L. E., Palmer, P., Lovas, F. J.,& Jewell, P. R. 2003b, ApJ, 596, L235

Hollis, J. M., Snyder, L. E., Suenram, R. D., & Lovas, F. J., 1980, ApJ, 241, 1001

Ilyushin, V.V., Alekseev, E.A., Dyubko, S.F, Podnos, S.V, Kleiner, I, Margules, L., Wlodarczak, G. Demaison, J., Cosleou, J., Mate, B., Karyakin, E. N., Golubiatnikov, G. Yu., Fraser, G.T., Suenram, R. D., & Hougen, J. T. 2001 J. Mol. Spectrosc. 205, 286

Jewell, P. R. 1990, Users Manual for the NRAO 12 m Millimeter-Wave Telescope, National Radio Astronomy Observatory publication

Jenkins, F. A., & White, H. E. 1957, Fundamentals of Optics (New York: McGraw-Hill)

Kaushik, V. K., Takagi, K., & Matsumura, C. 1980, J. Mol. Spectrosc. 82, 418

Kuan, Y.-J, Charnley, S. B., Huang, H.- C., Tseng, W.-L., & Kisiel, Z. 2003, ApJ, 593, 848

Kuan, Y., Mehringer, D. M., & Snyder, L. E. 1996, ApJ, 459, 619

Kutner, M. L., & Ulich, B. L. 1981, ApJ, 250, 341

Lis, D. C., Goldsmith, P. F., Carlstrom, J. E., & Scoville, N. Z. 1993, ApJ, 402, 238

Liu, S.-Y., Girart, J. M., Remijan, A., & Snyder, L. E. 2002, ApJ, 576, 255

Liu, S.-Y., Mehringer, D. M., & Snyder, L. E. 2001, ApJ, 552, 654

Liu, S.-Y., & Snyder, L. E. 1999, ApJ, 523, 683

Lovas, F.J., Kawashima, Y., Grabow, J.-U., Suenram, R.D., Fraser, G.T., & Hirota, E. 1995, ApJ, 455, L201

Mehringer, D.M., Pearson, J.C., Keene, J., & Phillips, T.G. 2004, ApJ, 608, 306

Nummelin, A., & Bergman, P. 1999, A&A, 341, L59

Nummelin, A.,Bergman, P., Hjalmarson,Å. , Friberg, P., Irvine, W.M., Millar, T.J., Ohishi, M., & Saito, S. 1998, ApJS, 117, 427.

Pei, C. C., Liu, S.-Y., & Snyder, L. E. (2000), ApJ, 530, 800

Reid, M. J., & Moran, J. M. 1988, in Galactic and Extragalactic Radio Astronomy, ed. G. L. Verschuur & K. I. Kellerman, (Berlin:Springer-Verlag), 255

Remijan, A., Snyder, L. E., Friedel, D. N., Liu, S.-Y., & Shah, R. Y. 2003, ApJ, 590, 314

Remijan, A., Snyder, L. E., Liu, S.-Y., Mehringer, D., & Kuan, Y.-J. 2002, ApJ, 576, 264

Rohlfs, K. & Wilson, T. L. 2000, Tools of Radio Astronomy (3rd ed.; Berlin: Springer), 141

Salter, C., Maddalena, R. J., & Garwood, B. 1995, The UniPOPS Cookbook (Greenbank:NRAO)

Schilke, P., Phillips, T. G., & N. Wang 1995, ApJ, 441, 334

Suenram, R. D., & Lovas, F. J. 1984, J. Mol. Spectrosc. 105, 351

Snyder, L. E. 1997, Orig. Life & Evol. Biosphere, 27, 115

Snyder, L. E., Hollis, J. M., Suenram, R. D., Lovas, F. J., Brown, L. W., & Buhl, D., 1983, ApJ, 268, 123

Snyder, L. E., Lovas, F. J., Mehringer, D. M., Miao, N. Y., Kuan, Y.-J., Hollis, J. M., & Jewell, P. R. 2002, ApJ, 578, 245

Snyder, L. E., Veal, J. M., Woodney, L. M., Wright, M. C. H., Palmer, P., A'Hearn, M. F., Kuan, Y.-J., de Pater, I, & Forster, J. R. 2001, AJ, 121, 1147

Suenram, R.D. & Lovas, F.J. 1980, J. Am. Chem. Soc. 102, 7180.

Suenram, R.D. & Lovas, F.J. 1984, J. Mol. Spectrosc. 105, 351

Taylor, B.N. & Kuyatt, C.E. 1994, NIST Tech. Note 1297, U.S. Govt. Printing Office, Washington, DC 20402

Townes, C. H., & Schawlow, A. L. 1975, Microwave Spectroscopy (New York: Dover), 94

Ulich, B. L., & Haas, R. W. 1975, ApJS, 30, 247

Sommerfeld, A. 1964, Optics (New York: Academic Press), 290

Watson, J.K.G. 1977, in Vibrational Spectra and Structure. A Series of Advances, Vol. 6, ed. J. R. Durig (New York: Elsevier), 19

Zmuidzinas, J., Blake, G. A., Carlstrom, J., Keene, J., & Miller, D. 1995, ApJ, 447, L125
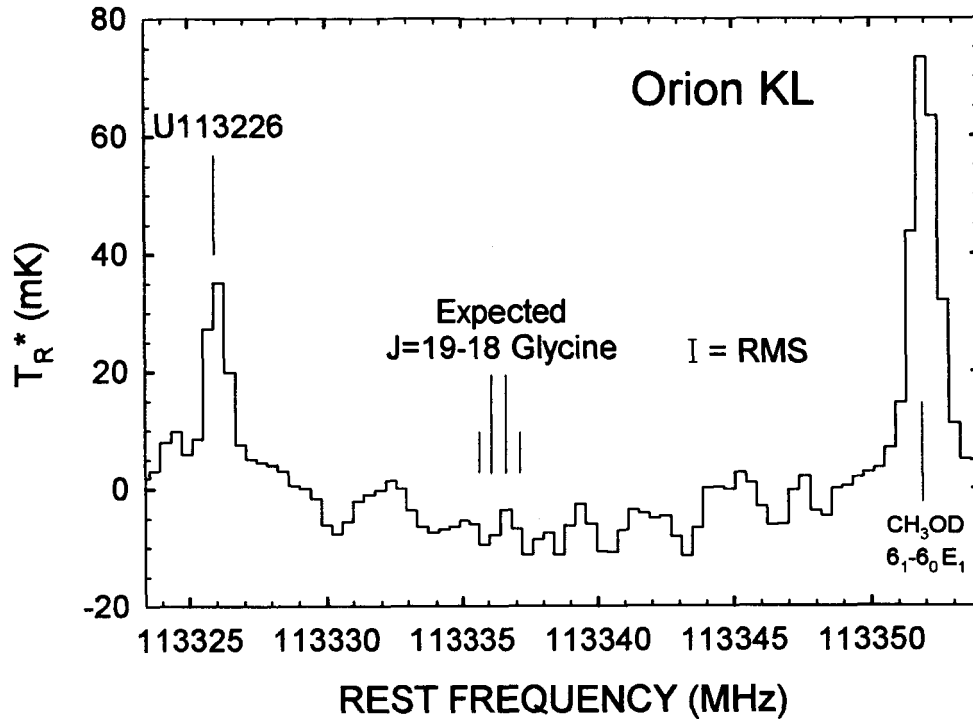

Fig. 1.— Orion KL spectra from 113,323 to 113,355 MHz (centered at 113,339 MHz) observed with the Hybrid Spectrometer on the NRAO 12 m. The spectral positions of the negative results for the nearly four-fold degenerate J = 19-18 glycine lines are marked by the four vertical lines centered at 113,336 MHz. U113.226 is on the left, and CH_3OD is on the right. The ordinate is in units of mK on the T_R^* scale. The abscissa is rest frequency calculated with respect to V_{LSR} = 9 km s^{-1} (for the Orion compact ridge) except the CH_3OD rest frequency is with respect to V_{LSR} = 5.6 km s^{-1} (representative of the Orion hot core). The rms noise level for the spectral region between U113.226 and CH_3OD is 3.7 mK.
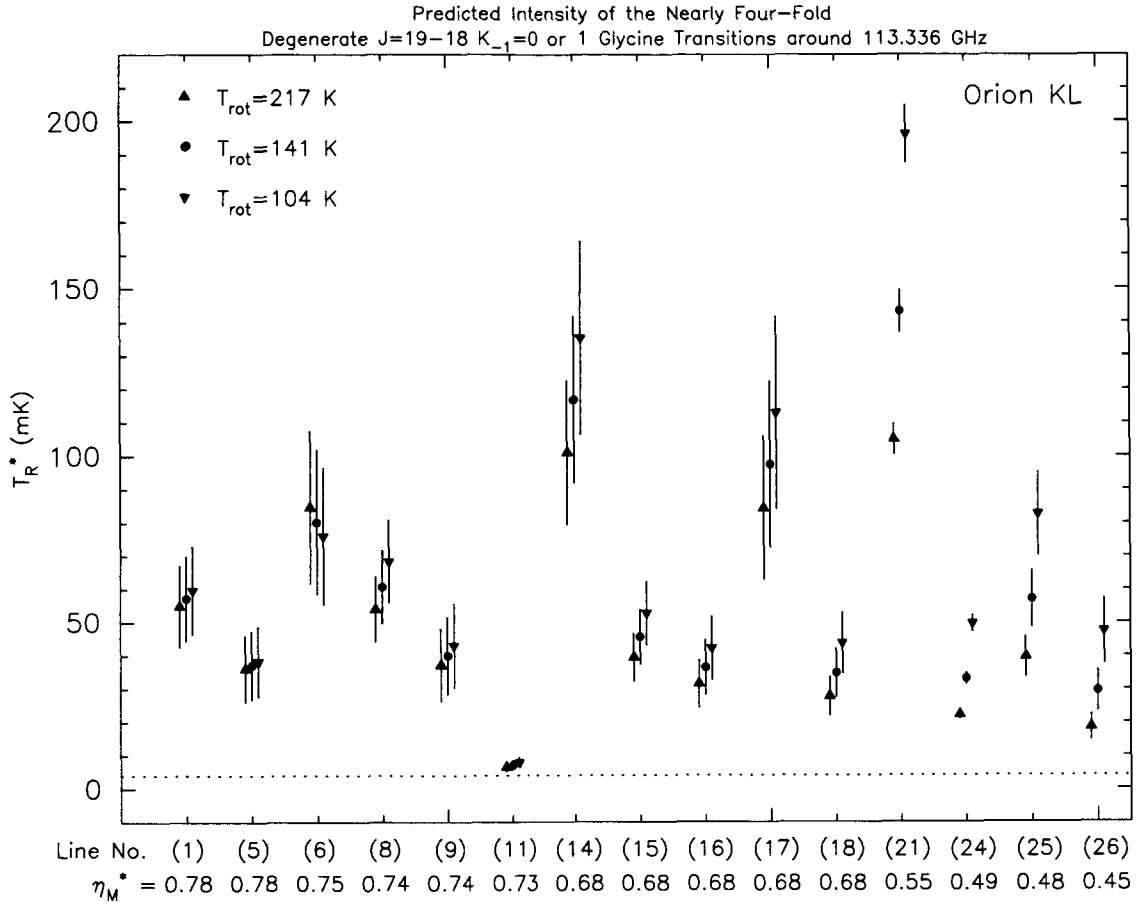
Fig. 2.— The intensity of each of the 15 Orion KL glycine lines reported by Kuan et al. (2003) was used to independently predict the intensity of the nearly four-fold degenerate J = 19-18 glycine lines at 113.366 GHz. A 45" extended source of glycine was assumed. As in Figure 1, the ordinate is in units of mK based on the T_R^* scale. The upper abscissa lists the glycine line number from Table 1, and the lower gives the corresponding main beam efficiency, η_M^*, for the NRAO 12 m. Each predicted intensity is calculated for the Orion rotational temperature and its uncertainties, $T_{rot} = 141^{+76}_{-37}$ K, derived by Kuan et al. (2003) ($\blacktriangle$ = 217 K; $\bullet$ = 141 K; $\blacktriangledown$ = 104 K). The uncertainties for each rotational temperature point are based on the rms noise level given for each glycine line reported by Kuan et al. (2003) (see Table 1). The dotted line shows the 3.7 mK noise level from Figure 1. The intensities predicted from all 15 reported glycine lines show that the 19-18 glycine lines should have been detected in Orion KL, but they were not (see Figure 1).
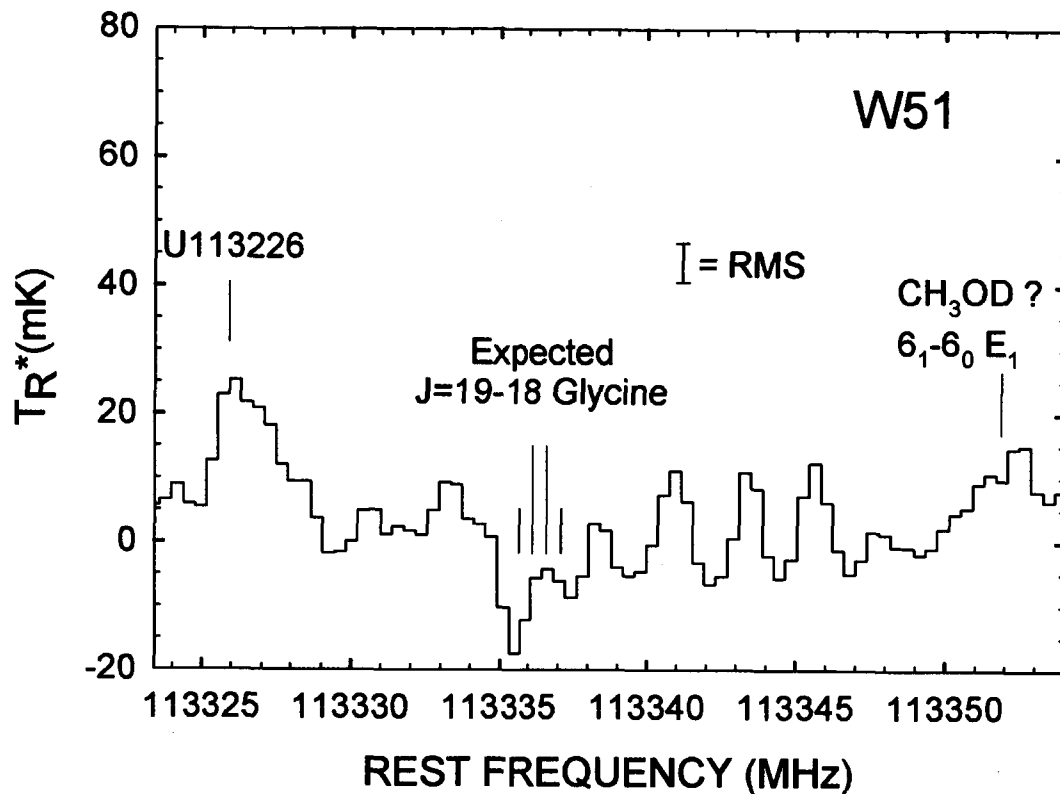
Fig. 3.— W51 spectra from 113,323 to 113,355 MHz (centered at 113,339 MHz) observed with the Hybrid Spectrometer on the NRAO 12 m. The spectral positions of the negative results for the nearly four-fold degenerate $J = 19$-18 glycine lines are marked by the four vertical lines centered at 113,336 MHz. U113.226 is on the left, and a weak emission feature from CH_3OD is on the right. As in Figure 1, the ordinate is in units of mK on the T_R^* scale. The abscissa is rest frequency calculated with respect to $V_{LSR} = 57.1$ km s^{-1}. The rms noise level for the spectral region between U113.226 and CH_3OD is 6.4 mK.
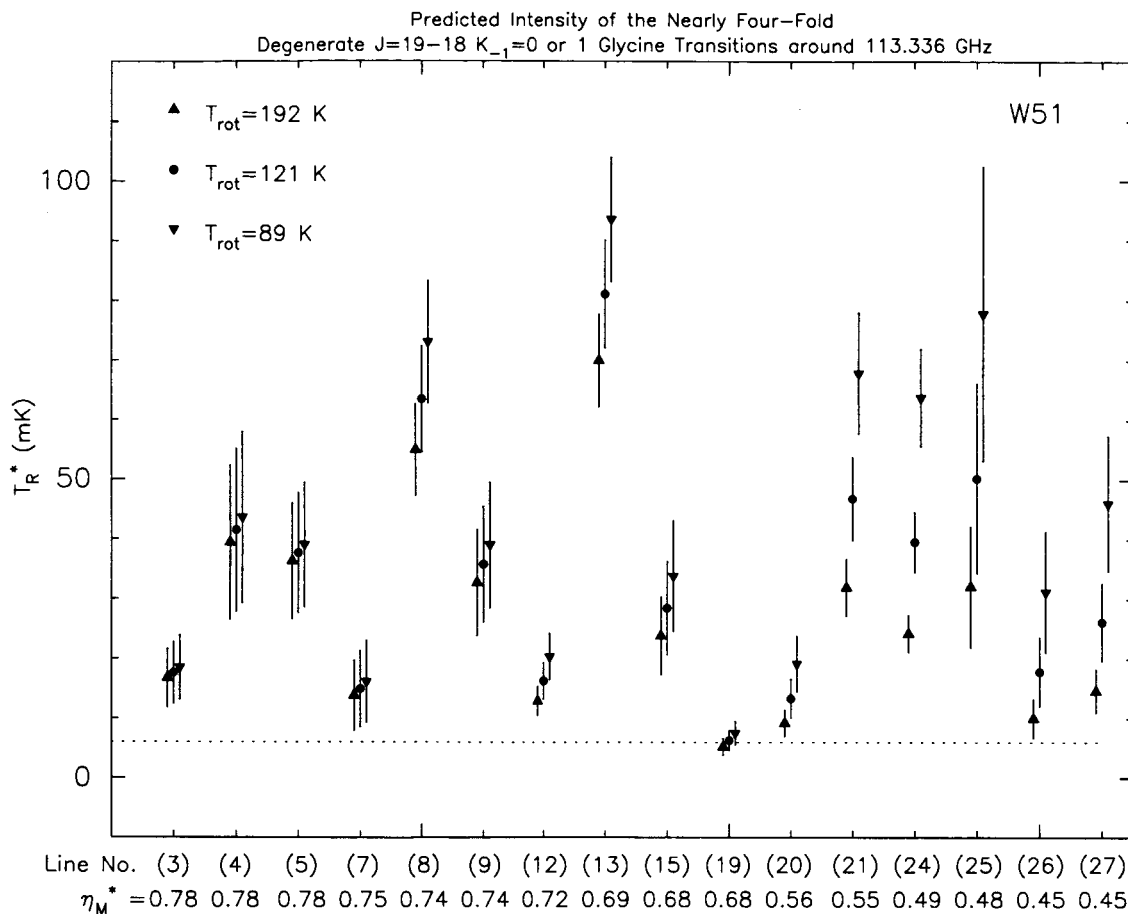
Fig. 4.— The intensity of each of the 16 W51 glycine lines reported by Kuan et al. (2003) was used to independently predict the intensity of the nearly four-fold degenerate J = 19-18 glycine lines at 113.366 GHz. A 45" extended source of glycine was assumed. As in Figure 1, the ordinate is in units of mK based on the T_R^* scale. The upper abscissa lists the glycine line number from Table 1, and the lower gives the corresponding main beam efficiency, η_M^*, for the NRAO 12 m. Each predicted intensity is calculated for the W51 rotational temperature and its uncertainties, $T_{rot} = 121_{-32}^{+71}$ K, derived by Kuan et al. (2003) ($\blacktriangle$ = 192 K; $\bullet$ = 121 K; $\blacktriangledown$ = 89 K). The uncertainties for each rotational temperature point are based on the rms noise level given for each glycine line reported by Kuan et al. (2003) (see Table 1). The dotted line shows the 6.4 mK noise level from Figure 3. The intensities predicted from 15 of the 16 reported glycine lines show that the 19-18 glycine lines should have been detected in W51, but they were not (see Figure 3).
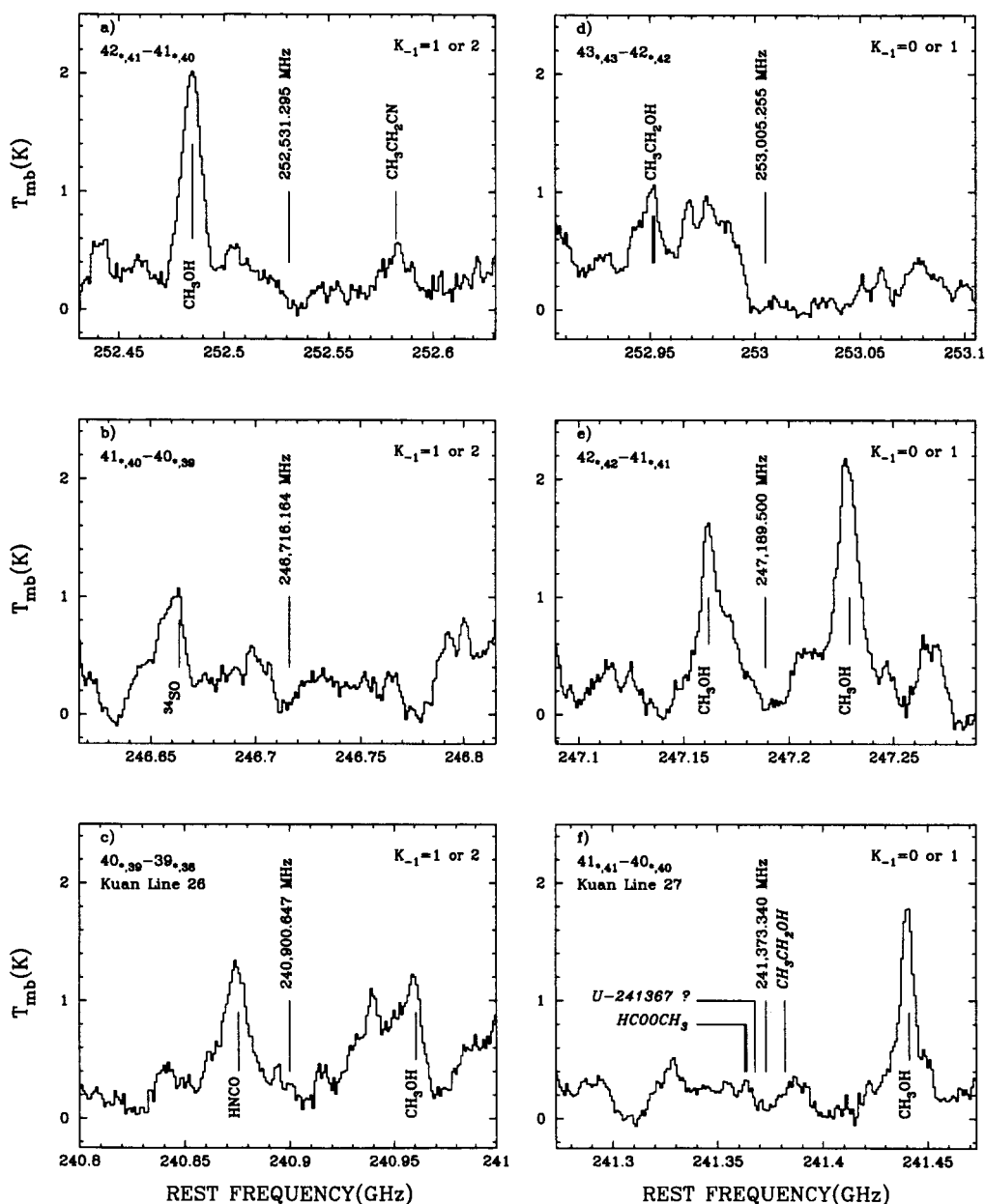
Fig. 5.— This figure is adapted from the Sgr B2(N) data and molecular assignments given by Nummelin et al. (1998). (a) The Nummelin et al. (1998) data for the missing glycine lines for the $K_{-1} = 1$ or 2 frequencies of the fourfold degenerate glycine quartet J = 42 - 41 at 252,531.295 MHz. (b) The missing fourfold degenerate glycine quartet J = 41 - 40 at 246,716.164 MHz. (c) The data for line 26 of Kuan et al. (2003), which is reported to be the fourfold degenerate glycine quartet J = 40 - 39 at 240,900.647 MHz. (d) The data for the missing glycine lines for the $K_{-1} = 0$ or 1 frequencies of the fourfold degenerate glycine quartet J = 43 - 42 at 253,005.255 MHz. (e) The missing fourfold degenerate glycine quartet J = 42 - 41 at 247,189.500 MHz. (f) The missing fourfold degenerate glycine quartet J = 41 - 40 at 241,373.340 MHz (line 27 of Kuan et al. 2003).
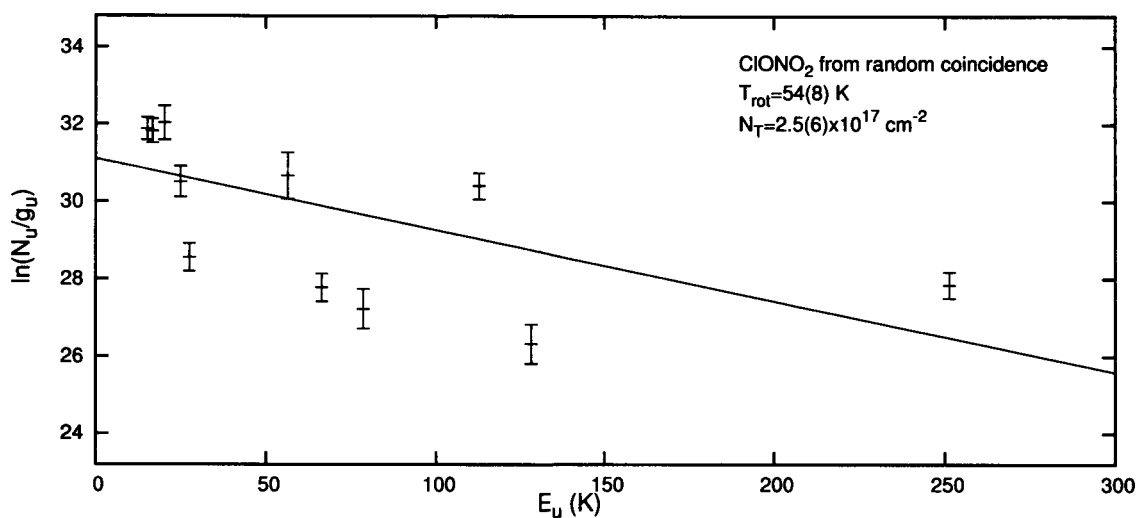
Fig. 6.— Rotational temperature diagram for chlorine nitrate ($ClONO_2$) constructed from randomly coincident unidentified lines detected in the direction of Sgr B2(N-LMH) by Friedel et al. (2004). The ordinate is the Naperian logarithm of the beam-averaged upper level column density, $< N_u >$, divided by g_u, the statistical weight of the upper level (2J+1); the abscissa E_u is the upper state rotational energy level for each transition. As discussed in the text, this diagram is not evidence supporting a detection of interstellar chlorine nitrate.
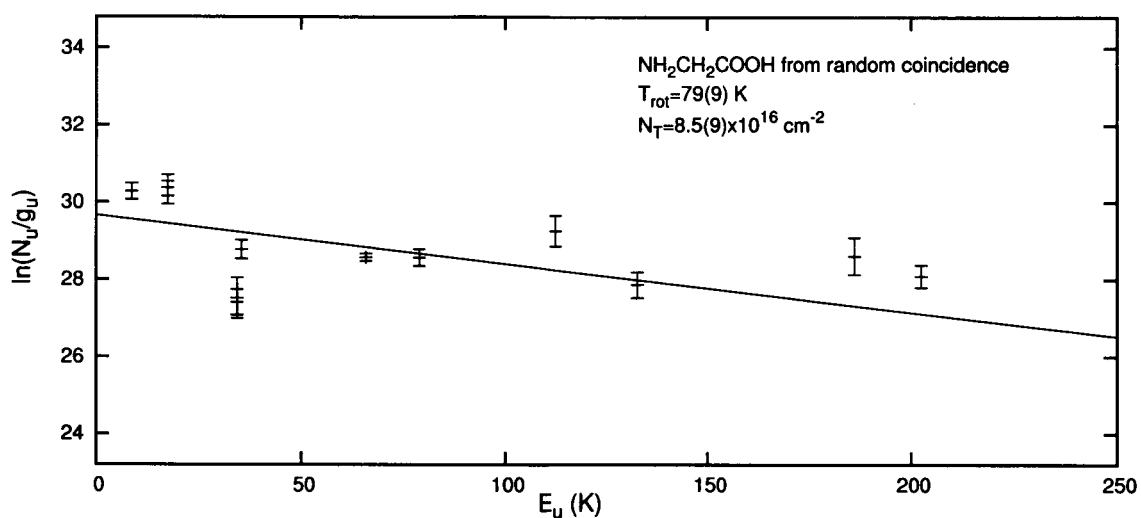
Fig. 7.— Rotational temperature diagram for glycine (NH$_2$CH$_2$COOH) constructed from randomly coincident unidentified lines detected in the direction of Sgr B2(N-LMH) by Friedel et al. (2004). The ordinate is the Naperian logarithm of the beam-averaged upper level column density, $< N_u >$, divided by g_u, the statistical weight of the upper level (2J+1); the abscissa E_u is the upper state rotational energy level for each transition. As discussed in the text, this diagram is not evidence supporting a detection of interstellar glycine.

Table 1. Summary of Reported Glycine Line Detections

Line No.	Transition	Type	Rest Frequency (MHz)[a]	S Line Strength	E_u (K)	Sgr B2(N-LMH) v_{LSR} (km s^{-1})[b]	Sgr B2(N-LMH) T^*_R (mK)[c]	Orion-KL v_{LSR} (km s^{-1})[b]	Orion-KL T^*_R (mK)[c]	W51 e1/e2 v_{LSR} (km s^{-1})[b]	W51 e1/e2 T^*_R (mK)[c]
1	$21_{1,20} - 20_{2,19}$	b	130346.775(13)	16.7	72.3	66.3(1.2)	26.0(5.9)	8.0(3.1)	9.0(2.0)	U-Interloper[d]	
2	$21_{2,20} - 20_{2,19}$	a	130354.371(13)	20.5	72.3	66.3(1.2)	30.0(5.9)	U-Interloper		U-Interloper	
3	$21_{1,20} - 20_{1,19}$	a	130360.890(13)	20.5	72.3	U-Interloper		U-Interloper		60.0(3.1)	7.5(2.2)
4	$21_{2,20} - 20_{1,19}$	b	130368.485(13)	16.7	72.3	ID-Interloper[e]		ID-Interloper		60.0(3.1)	6.4(2.1)
5	$19_{3,16} - 18_{3,15}$	a	131423.627(13)	18.1	67.6	Not Observed[f]		8.5(1.1)	15.0(4.1)	60.0(3.0)	15.0(4.0)
6	$12_{5,8} - 11_{4,7}$	b	142225.340(120)	4.6	34.0	64.0(5.6)	22.0(2.0)	7.8(2.8)	5.2(1.4)	Not Detected[g]	
7	$21_{3,18} - 20_{3,17}$	a	142301.054(13)	20	81.0	64.0(2.1)	38.0(2.2)	ID-Interloper		60.0(2.8)	6.6(2.8)
8	$21_{9,12} - 20_{9,11}$	a	144841.736(22)	17.2	102.9	Not Observed		5.0(2.8)	20.9(3.8)	56.0(2.8)	20.7(2.9)
9	$21_{5,17} - 20_{5,16}$	a	144847.191(16)	19.7	84.8	Not Observed		8.0(1.4)	17.9(5.2)	60.0(1.4)	15.5(4.2)
10	$24_{1,23} - 23_{2,22}$	b	147812.030(17)	19.7	92.7	64.0(1.0)	20.0(5.0)	Not Observed		Not Observed	
	$24_{2,23} - 23_{2,22}$	a	147813.168(17)	23.5	"						
	$24_{1,23} - 23_{1,22}$	a	147814.186(17)	"	"						
	$22_{3,19} - 21_{3,18}$	a	147815.031(14)	21	88.0						
	$24_{2,23} - 23_{1,22}$	b	147815.324(17)	19.7	92.7						
11	$25_{0,25} - 24_{1,24}$	b	148268.007(18)	23.6	94.0	U-Interloper		5.0(2.0)	11.0(2.1)	U-Interloper	
	$25_{1,25} - 24_{1,24}$	a	148268.016(18)	24.8	"						
	$25_{0,25} - 24_{0,24}$	a	148268.024(18)	"	"						
	$25_{1,25} - 24_{0,24}$	b	148268.033(18)	23.6	"						
12	$22_{12,11} - 21_{12,10}$	a	150909.703(20)	15.5	130.8	68.0(2.7)	18.0(2.5)	Not Detected(S/N)[h]		58.0(2.0)	8.0(1.5)
	$22_{12,10} - 21_{12,9}$	a	"	"	"						
13	$23_{6,18} - 22_{6,17}$	a	160153.431(30)	21.4	103.5	U-Interloper		U-Interloper		60.0(2.5)	37.0(4.1)
14	$26_{2,24} - 25_{3,23}$	b	164851.728(30)	18.8	113.7	Not Observed		7.5(1.2)	21.2(4.5)	U-Interloper	
15	$26_{3,24} - 25_{3,23}$	a	164862.039(30)	25.2	113.7	Not Observed		7.5(1.2)	25.0(4.5)	60.0(1.2)	14.6(4.0)
16	$26_{2,24} - 25_{2,23}$	a	164870.438(30)	25.2	113.7	Not Observed		7.5(1.2)	20.0(4.5)	Not Detected	
17	$26_{3,24} - 25_{2,23}$	b	164880.749(30)	18.8	113.7	Not Observed		7.5(1.2)	17.7(4.5)	Not Detected(S/N)	
18	$24_{12,13} - 23_{12,12}$	a	164886.068(33)	18.0	146.4	Not Observed		7.5(1.2)	21.6(4.5)	Not Detected	
	$24_{12,12} - 23_{12,11}$	a	164886.071(33)	"	"						
19	$27_{1,26} - 26_{2,25}$	b	165270.666(22)	22.7	115.7	64.8(0.9)	60.0(4.6)	Not Detected		58.2(2.4)	8.0(2.1)
	$27_{2,26} - 26_{2,25}$	a	165270.829(22)	26.5	"						
	$27_{1,26} - 26_{1,25}$	a	165270.979(22)	"	"						
	$27_{2,26} - 26_{1,25}$	b	165271.142(22)	22.7	"						
20	$33_{2,31} - 32_{3,30}$	b	205560.595(67)	25.7	176.8	67.0(0.7)	95.0(11.9)	Not Detected		58.6(3.9)	17.0(4.1)
	$33_{3,31} - 32_{3,30}$	a	205560.730(67)	32.2	"						
	$33_{2,31} - 32_{2,30}$	a	205560.849(67)	"	"						
	$33_{3,31} - 32_{2,30}$	b	205560.984(67)	25.7	"						
21	$35_{0,35} - 34_{1,34}$	b	206468.453(17)	33.6	180.5	66.0(1.9)	210.0(8.9)	7.3(0.7)	230.0(10.0)	60.5(0.7)	65.0(9.7)
	$35_{1,35} - 34_{1,34}$	a	"	34.8	"						
	$35_{0,35} - 34_{0,34}$	a	"	"	"						
	$35_{1,35} - 34_{0,34}$	b	"	33.6	"						
22	$36_{0,36} - 35_{1,35}$	b	212286.829(18)	34.6	190.7	66.0(0.7)	58.0(15.6)	ID-Interloper		ID-Interloper	
	$36_{1,36} - 35_{1,35}$	a	"	35.8	"						
	$36_{0,36} - 35_{0,35}$	a	"	"	"						
	$36_{1,36} - 35_{0,35}$	b	"	34.6	"						
23	$36_{2,34} - 35_{3,33}$	b	223004.375(88)	28.9	208.2	67.3(1.8)	40.0(10.5)	Not Detected		Not Observed	
	$36_{3,34} - 35_{3,33}$	a	223004.395(88)	35.2	"						
	$36_{2,34} - 35_{2,33}$	a	223004.413(88)	"	"						
	$36_{3,34} - 35_{2,33}$	b	223004.432(88)	28.9	"						
24	$36_{3,33} - 35_{4,32}$	b	228419.435(104)	25.9	216.3	65.0(1.3)	70.0(7.6)	4.9(3.5)	40.0(2.0)	57.0(1.8)	40.0(5.1)
	$36_{4,33} - 35_{4,32}$	a	228420.029(104)	34.9	"						
	$36_{3,33} - 35_{3,32}$	a	228420.526(104)	"	"						
	$36_{4,33} - 35_{3,32}$	b	228421.120(104)	25.9	"						
25	$33_{6,27} - 32_{6,26}$	a	230348.993(64)	31.3	202.5	ID-Interloper		8.0(3.5)	26.0(3.9)	58.7(3.5)	19.0(6.0)
26	$40_{1,39} - 39_{2,38}$	b	240900.647(76)	35.8	244.2	63.2(0.6)	94.0(11.0)	5.0(1.7)	35.0(7.2)	57.0(1.7)	17.0(5.5)
	$40_{2,39} - 39_{2,38}$	a	"	39.5	"						
	$40_{1,39} - 39_{1,38}$	a	"	"	"						
	$40_{2,39} - 39_{1,38}$	b	"	35.8	"						
27	$41_{0,41} - 40_{1,40}$	b	241373.340(32)	39.6	245.9	U/ID-Interloper		Not Detected		57.0(1.7)	26.0(6.4)
	$41_{1,41} - 40_{1,40}$	a	"	40.8	"						
	$41_{0,41} - 40_{0,40}$	a	"	"	"						
	$41_{1,41} - 40_{0,40}$	b	"	39.6	"						

[a]2σ frequency uncertainty is in parentheses.

[b]This is the v_{LSR} and uncertainty listed by Kuan et al. (2003).

[c]This is the T^*_R and rms noise level listed by Kuan et al. (2003).

[d]This indicates that there was an unidentified interloper.

[e]This indicates that there was an identified interloper.

[f]This indicates that no observations were made toward this source for this transition.

[g]This indicates that this line toward this source was not detected but should have been (the predicted signal should have been more than 3σ).

[h]This indicates that this line toward this source was not detected because it's predicted strength should have been below 3σ.

Table 2.   113 GHz Search Frequencies for Orion KL and W51

Rest Frequency (MHz)[a]	Molecule	Transition	Type	S Line Strength	E_u (K)	Orion-KL T_R^* (mK)	Orion-KL Δv (km s^{-1})	W51 e1/e2 T_R^* (mK)	W51 e1/e2 Δv (km s^{-1})
113,326	U113.326	···	···	···	···	36	1.6	23	2.9
113,335.700 (18)	NH_2CH_2COOH	$19_{0,19} - 18_{1,18}$	b	17.6	55.5	< 3.7	···	< 6.4	···
113,336.209 (18)	NH_2CH_2COOH	$19_{1,19} - 18_{1,18}$	a	18.8	55.5	< 3.7	···	< 6.4	···
113,336.696 (18)	NH_2CH_2COOH	$19_{0,19} - 18_{0,18}$	a	18.8	55.5	< 3.7	···	< 6.4	···
113,337.205 (18)	NH_2CH_2COOH	$19_{1,19} - 18_{0,18}$	b	17.6	55.5	< 3.7	···	< 6.4	···
113,250.80 (10)[b]	CH_3OD	$6_1 - 6_0 E_1$	b	7.8[c]	54.8	74	1.4	11	3.6

[a] 2σ uncertainty is in parentheses.

[b] Rest Frequency from Kaushik, Takage, & Matsumura (1980)

[c] This is the product $S\mu^2$ in Debyes^2.

Table 3. Connected $K_{-1}=1$ or 2 Glycine Transitions in the Nummelin et al. Survey Range

Transition	Type	Rest Frequency (MHz)[a]	S Line Strength	E_u (K)	Predicted T_{mb} (mK)	Observed T_{mb} (mK)	Comments
$43_{2,42} - 42_{2,41}$	a	258,346.029 (96)	42.5	276.8	$\cdots$	$\cdots$	Masked by CH_3NH_2 at 258,349 MHz[b]
$43_{2,42} - 42_{1,41}$	b	258,346.029 (96)	38.8	276.8			
$43_{1,42} - 42_{2,41}$	b	258,346.029 (96)	38.8	276.8			
$43_{1,42} - 42_{1,41}$	a	258,346.029 (96)	42.5	276.8			
$42_{2,41} - 41_{2,40}$	a	252,531.295 (89)	41.5	268.2	233^{+65}_{-55}	< 100	
$42_{1,41} - 41_{2,40}$	b	252,531.295 (89)	37.8	268.2			
$42_{2,41} - 41_{1,40}$	b	252,531.295 (89)	37.8	268.2			
$42_{1,41} - 41_{1,40}$	a	252,531.295 (89)	41.5	268.2			
$41_{2,40} - 40_{2,39}$	a	246,716.164 (82)	40.5	256.1	265^{+58}_{-53}	< 100	
$41_{2,40} - 40_{1,39}$	b	246,716.164 (82)	36.8	256.1			
$41_{1,40} - 40_{2,39}$	b	246,716.164 (82)	36.8	256.1			
$41_{1,40} - 40_{1,39}$	a	246,716.164 (82)	40.5	256.1			
$40_{2,39} - 39_{2,38}$	a	240,900.647 (76)	39.5	244.3	Std[c]	300	Line 26[d]
$40_{1,39} - 39_{2,38}$	b	240,900.647 (76)	35.8	244.3			
$40_{2,39} - 39_{1,38}$	b	240,900.647 (76)	35.8	244.3			
$40_{1,39} - 39_{1,38}$	a	240,900.647 (76)	39.5	244.3			
$39_{2,38} - 38_{2,37}$	a	235,084.758 (70)	38.5	232.7	338^{+73}_{-68}	250	Line U235.085 at 235,085 MHz[b]
$39_{2,38} - 38_{1,37}$	b	235,084.758 (70)	34.8	232.7			
$39_{1,38} - 38_{2,37}$	b	235,084.758 (70)	34.8	232.7			
$39_{1,38} - 38_{1,37}$	a	235,084.758 (70)	38.5	232.7			
$38_{2,37} - 37_{2,36}$	a	229,268.511 (65)	37.5	221.4	$\cdots$	$\cdots$	Masked by CH_3CH_2CN at 229,262 MHz[b]
$38_{1,37} - 37_{2,36}$	b	229,268.511 (65)	33.8	221.4			
$38_{2,37} - 37_{1,36}$	b	229,268.511 (65)	33.8	221.4			
$38_{1,37} - 37_{1,36}$	a	229,268.511 (65)	37.5	221.4			
$37_{2,36} - 36_{2,35}$	a	223,451.918 (60)	36.5	210.4	$\cdots$	$\cdots$	Masked by NH_2CHO at 223,449 MHz[b]
$37_{2,36} - 36_{1,35}$	b	223,451.918 (60)	32.8	210.4			
$37_{1,36} - 36_{2,35}$	b	223,451.918 (60)	32.8	210.4			
$37_{1,36} - 36_{1,35}$	a	223,451.918 (60)	36.5	210.4			

[a] 2σ uncertainty is in parentheses.

[b] Nummelin et al. (1998)

[c] The intensity of this line is the standard on which all other Table 3 and Table 4 predictions are based.

[d] Kuan et al. (2003) list this as glycine line 26.

Table 4. Connected $K_{-1}=0$ or 1 Glycine Transitions in the Nummelin et al. Survey Range

Transition	Type	Rest Frequency (MHz)[a]	S Line Strength	E_u (K)	Predicted T_{mb} (mK)	Observed T_{mb} (mK)	Comments
$44_{1,44} - 43_{1,43}$	a	258,820.597 (46)	43.8	282.3	210^{+72}_{-57}	< 200	Dominated by narrow noise spikes.[b]
$44_{1,44} - 43_{0,43}$	b	258,820.597 (46)	42.6	282.3			
$44_{0,44} - 43_{1,43}$	b	258,820.597 (46)	42.6	282.3			
$44_{0,44} - 43_{0,43}$	a	258,820.597 (46)	43.8	282.3			
$43_{1,43} - 42_{1,42}$	a	253,005.255 (41)	42.8	269.9	240^{+68}_{-57}	< 50	
$43_{0,43} - 42_{1,42}$	b	253,005.255 (41)	41.6	269.9			
$43_{1,43} - 42_{0,42}$	b	253,005.255 (41)	41.6	269.9			
$43_{0,43} - 42_{0,42}$	a	253,005.255 (41)	42.8	269.9			
$42_{1,42} - 41_{1,41}$	a	247,189.500 (36)	41.8	257.7	273^{+62}_{-57}	< 100	
$42_{1,42} - 41_{0,41}$	b	247,189.500 (36)	40.6	257.7			
$42_{0,42} - 41_{1,41}$	b	247,189.500 (36)	40.6	257.7			
$42_{0,42} - 41_{0,41}$	a	247,189.500 (36)	41.8	257.7			
$41_{1,41} - 40_{1,40}$	a	241,373.340 (32)	40.8	245.9	310^{+54}_{-53}	< 100	Line 27[c] Not masked by interlopers.[b]
$41_{0,41} - 40_{1,40}$	a	241,373.340 (32)	39.6	245.9			
$41_{1,41} - 40_{0,40}$	b	241,373.340 (32)	39.6	245.9			
$41_{0,41} - 40_{0,40}$	a	241,373.340 (32)	40.8	245.9			
$40_{1,40} - 39_{1,39}$	a	235,556.787 (29)	39.8	234.3	$\cdots$	$\cdots$	Masked by CH_3CH_2CN at 235,562 MHz.[b]
$40_{1,40} - 39_{0,39}$	b	235,556.787 (29)	38.6	234.3			
$40_{0,40} - 39_{1,39}$	b	235,556.787 (29)	38.6	234.3			
$40_{0,40} - 39_{0,39}$	a	235,556.787 (29)	39.8	234.3			
$39_{1,39} - 38_{1,38}$	a	229,739.850 (26)	38.8	223.0	$\cdots$	$\cdots$	Masked by CH_3OH at 229,756 MHz.[b]
$39_{0,39} - 38_{1,38}$	b	229,739.850 (26)	37.6	223.0			
$39_{1,39} - 38_{0,38}$	b	229,739.850 (26)	37.6	223.0			
$39_{0,39} - 38_{0,38}$	a	229,739.850 (26)	38.8	223.0			
$38_{1,38} - 37_{1,37}$	a	223,922.537 (23)	37.8	211.9	$\cdots$	$\cdots$	Masked by CH_3CH_2CN at 223,932 MHz.[b]
$38_{1,38} - 37_{0,37}$	b	223,922.537 (23)	36.6	211.9			
$38_{0,38} - 37_{1,37}$	b	223,922.537 (23)	36.6	211.9			
$38_{0,38} - 37_{0,37}$	a	223,922.537 (23)	37.8	211.9			

[a]2σ uncertainty is in parentheses.

[b]Nummelin et al. (1998)

[c]Kuan et al. (2003) list this as glycine line 27.

Table 5.   Other Candidates for Some of the Reported Glycine Lines

Line No.	Reported Frequency (MHz)	Possible Carrier	Transition	Carrier Rest Frequency (MHz)[a]	Source
6	142,225.4	HCOOCH$_3$	$16_{1,15}$-$16_{0,16}$	142,229.23(12)	Sgr B2(N), Orion
7	142,300.8	CH$_2$CDCN	$15_{2,13}$-$14_{2,12}$	142,304.59(1)	Sgr B2(N),W51
7	142,300.8	H$_2$CCCC	$16_{1,16}$-$15_{1,15}$	142,297.60(3)	Sgr B2(N),W51
8	144,841.8	c-C^{13}CCH$_2$	$18_{15,4}$-$8_{14,5}$	144,839.15(8)	Orion, W51
10	147,813.9[b]	g-CH$_3$CH$_2$OH	$21_{4,17}$-$20_{5,16}$	147,815.83(2)	Sgr B2(N)
12	150,909.8	CH$_2$DCH$_2$CN	$4_{3,1}$-$3_{2,2}$	150,910.45(12)	Sgr B2(N), Orion
13	160,153.5	CH$_3$CH$_2$CN	$35_{6,29}$-$36_{5,32}$ ν_{15}=1	160,154.1(26)	W51
13	160,153.5	(CH$_3$)$_2$CO	$21_{3,18}$-$21_{2,19}$ AE,EA	160,155.80(10)	W51
16	164,870.0	(CH$_3$)$_2$CO	$31_{12,19}$-$31_{11,20}$ EE	164,870.14(18)	Orion
16	164,870.0	(CH$_3$)$_2$CO	$31_{13,19}$-$31_{12,20}$ EE	164,870.14(8)	Orion
21	206,468.0	CH$_3$CH$_2$CN	$23_{6,18}$-$22_{6,17}$ ν_b=1	206,467.17(1)	Sgr B2(N), Orion, W51
21	206,468.0	CH$_3$CH$_2$CN	$23_{6,17}$-$22_{6,16}$ ν_b=1	206,467.31(1)	Sgr B2(N), Orion, W51
24	228,418.8	CH$_2$CHCN	$24_{11,13}$-$23_{11,12}$ ν_{15}=1	228,418.10(17)	Sgr B2(N), Orion, W51
24	228,418.8	CH$_2$CHCN	$24_{11,14}$-$23_{11,13}$ ν_{15}=1	228,418.10(17)	Sgr B2(N), Orion, W51

[a]2σ uncertainty is in parentheses.

[b]The line 10 spectra weren't displayed by Kuan et al. (2003), so this glycine frequency was selected from near the inferred line center.

Table 6. Lines Used for Random Coincidence Rotational Temperature Diagrams

Calculated Frequency (MHz)[a]	Corresponding Transition	Coincidental U Line (MHz)	Notes
Chlorine Nitrate ($^{35}ClNO_3$)			False Identificaion
85,910.164(620)	$11_{5,7} - 11_{4,9}$	U85,910.5	
85,917.061(30)	$17_{8,10} - 16_{8,9}$	"	
85,913.063(30)	$17_{8,9} - 16_{8,8}$	"	
86,001.262(30)	$17_{7,11} - 16_{7,10}$	none	31σ degenerate line pair should have been detected.
86,001.335(30)	$17_{7,10} - 16_{7,9}$	"	"
86,011.828(621)	$10_{5,6} - 10_{4,7}$	U86,010.0	
86,137.564(31)	$17_{6,12} - 16_{6,11}$	none	20σ line should have been detected.
86,140.166(31)	$17_{6,11} - 16_{6,10}$	none	20σ line should have been detected.
86,147.487(622)	$8_{5,3} - 8_{4,4}$	U86,148.0	
86,152.956(622)	$8_{5,4} - 8_{4,5}$	U86,151.6	
86,226.321(623)	$6_{5,1} - 6_{4,2}$	U86,226.5	
86,226.823(623)	$6_{5,2} - 6_{4,3}$	"	
86,245.913(623)	$5_{5,0} - 5_{4,1}$	U86,248.2	
86,246.014(623)	$5_{5,1} - 5_{4,2}$	"	
86,405.625(32)	$17_{5,12} - 16_{5,11}$	none	26σ line should have been detected.
86,491.659(33)	$17_{4,14} - 16_{4,13}$	none	26σ line should have been detected.
86,941.598(1033)	$43_{6,37} - 43_{5,38}$	U86,944.5	
86,942.770(476)	$29_{3,26} - 29_{3,27}$	"	
106,300.938(29)	$21_{8,14} - 20_{8,13}$	none	17σ degenerate line pair should have been detected.
106,300.938(29)	$21_{8,13} - 20_{8,12}$	"	"
106,467.629(31)	$21_{7,15} - 20_{7,14}$	U106,468.5	
106,468.848(31)	$21_{7,14} - 20_{7,13}$	"	
106,469.725(454)	$31_{4,28} - 31_{3,29}$	"	
106,863.802(34)	$21_{4,18} - 20_{4,17}$	none	11σ line should have been detected.
Glycine (NH_2CH_2COOH)			False Identificaion
86,210.408(367)	$19_{7,13} - 19_{6,14}$	U86,207.8	
86,440.861(1000)	$32_{9,23} - 32_{8,24}$	U86,440.2	
86,885.889(19)	$12_{3,9} - 11_{3,8}$	none	14σ line should have been detected.
89,735.673(344)	$26_{7,20} - 26_{6,21}$	U89,731.5	
89,831.975(10)	$14_{1,13} - 13_{1,12}$	U89,829.6	
89,875.646(367)	$8_{7,1} - 8_{6,2}$	none	10σ line should have been detected.
90,035.981(16)	$15_{0,15} - 14_{1,14}$	U90,033.9	
90,043.198(16)	$15_{1,15} - 14_{1,14}$	none	19σ line should have been detected.
90,049.762(16)	$15_{0,15} - 14_{0,14}$	none	19σ line should have been detected.
90,056.980(100)	$15_{1,15} - 14_{0,14}$	none	9σ line should have been detected.
90,303.355(12)	$14_{2,13} - 13_{1,12}$	U90,304.8	
106,559.495(497)	$24_{6,18} - 23_{7,17}$	U106,559.8	
106,767.076(788)	$31_{8,24} - 30_{9,21}$	U106,763.3	
109,960.322(11)	$16_{8,9} - 15_{8,8}$	U109,959.6	
109,961.001(11)	$16_{8,8} - 15_{8,7}$	"	
110,089.888(121)	$7_{5,3} - 6_{4,2}$	U110,085.6	
110,104.790(74)	$4_{4,0} - 3_{2,1}$	U110,104.7	
110,106.688(121)	$7_{5,2} - 6_{4,3}$	"	

[a]2σ frequency uncertainty in parenthesis.